THESIS FOR THE DEGREE OF DOCTOR OF PHILOSOPHY (Ph.D.)

Role of poly(ADP-ribose) polymerase (PARP)-2 in mitochondrial metabolism and in doxorubicin-induced vascular damage

by

Magdolna Szántó

Supervisor: Dr. Péter Bay

UNIVERSITY OF DEBRECEN

DOCTORAL SCHOOL OF MOLECULAR MEDICINE

DEBRECEN, 2012.

1. TABLE OF CONTENT

2. ABBREVIATIONS

ACOX1	acyl-coenzyme A oxidase 1
AIF	apoptosis-inducing factor
AMPK	AMP-activated protein kinase
aP2	adipocyte protein 2
ATM	ataxia telangiectasia mutated gene
ATP	adenosine triphosphate
ATP5g1	ATP synthase, H^+ transporting, mitochondrial F0 complex, subunit c1
BER	base excision repair
BSA	bovine serum albumine
BTF	Bcl-2 associated transcription factor
CENP	centromere protein
COXIV	cytochrome c oxidase subunit IV
Cyt C	cytochrom c
DEMEM	Dulbecco's modified eagle medium
DOX	doxorubicin
DSE	dermatan sulfate epimerase
DTT	dithiotreitol
ECL	enhanced chemiluninescence
EDTA	ethylene-diamine tertaacetic acid
EE	energy expenditure
ERα	estrogen receptor α
FAS	fatty acid synthase
FOXO	forkhead box O
HBSS	Hank's balanced salt solution
HEPES	4-(2-hydroxyethyl)-1-piperazineethanesulfonic acid
HFD	high-fat diet
HP1α	heterochromatin protein 1α
HSPA2	heat shock-related 70 kDa protein 2
iNOS	inducible nitric oxide synthase
IL-1β	interleukin-1β

LPL	lipoprotein lipase
NAD^+	nicotinamide adenine dinucleotide
MCAD	medium chain acyl-CoA dehydrogenase
MCD	malonyl-CoA decarboxylase
MEF	mouse embryonic fibroblast
MMP	matrix metalloproteinase
Ndufa2	NADH dehydrogenase (ubiquinone) 1 alpha subcomplex subunit 2
Ndufb5	NADH dehydrogenase (ubiquinone) 1 beta subcomplex subunit 5
Oct-1	octamer-binding transcription factor-1
ONPG	ortho-nitrophenyl-β-D-galactopyranoside
PAR	poly(ADP-ribose)
PARylation	poly(ADP-ribosyl)ation
PARG	poly(ADP-ribose) glycohydrolase
PARP	poly(ADP-ribose) polymerase
PBS	phosphate buffered saline
PEI	polyethyleneimine
PGC-1α	peroxisome proliferator-activated receptor gamma coactivator 1-α
PIPES	piperazine-N,N'-bis(2-ethanesulfonic acid)
PMS	phenazine methosulphate
PPAR	peroxisome proliferator-activated receptor
RXR	retinoid X receptor
SDS	sodium dodecyl sulphate
SIRT	silent information regulator protein, sirtuin
SSB	single-strand break
SSBR	single-strand break repair
STAT1	signal transducer and activator of transcription 1
TBS	tris-buffered saline
TCA	trichloroacetic acid
TIF1β	transcriptional intermediary factor 1β
TMRE	tetramethylrhodamine ethyl ester
TNFα	tumor necrosis factor α
TP2	transition protein 2

TTF1	thyroid transcription factor-1
UCP2	uncoupling protein 2
WAT	white adipose tissue
XRCC1	x-ray repair cross-complementing protein

3. INTRODUCTION

3.1. The PARP superfamily

Poly(ADP-ribosyl)ation (PARylation) is a transient post-translational modification of proteins carried out by the poly(ADP-ribose) polymerase (PARP) enzymes. This is a dynamic process during which the enzymes catalyze the formation of ADP-ribose polymers onto different acceptor proteins using NAD^+ as a substrate. The PARP superfamily has 17 members in humans, encoded by different genes. PARP enzymes share a conserved catalytic domain that contains the PARP signature motif, a highly conserved sequence that forms the active site (Amé et al., 2004) (**Figure 1.**).

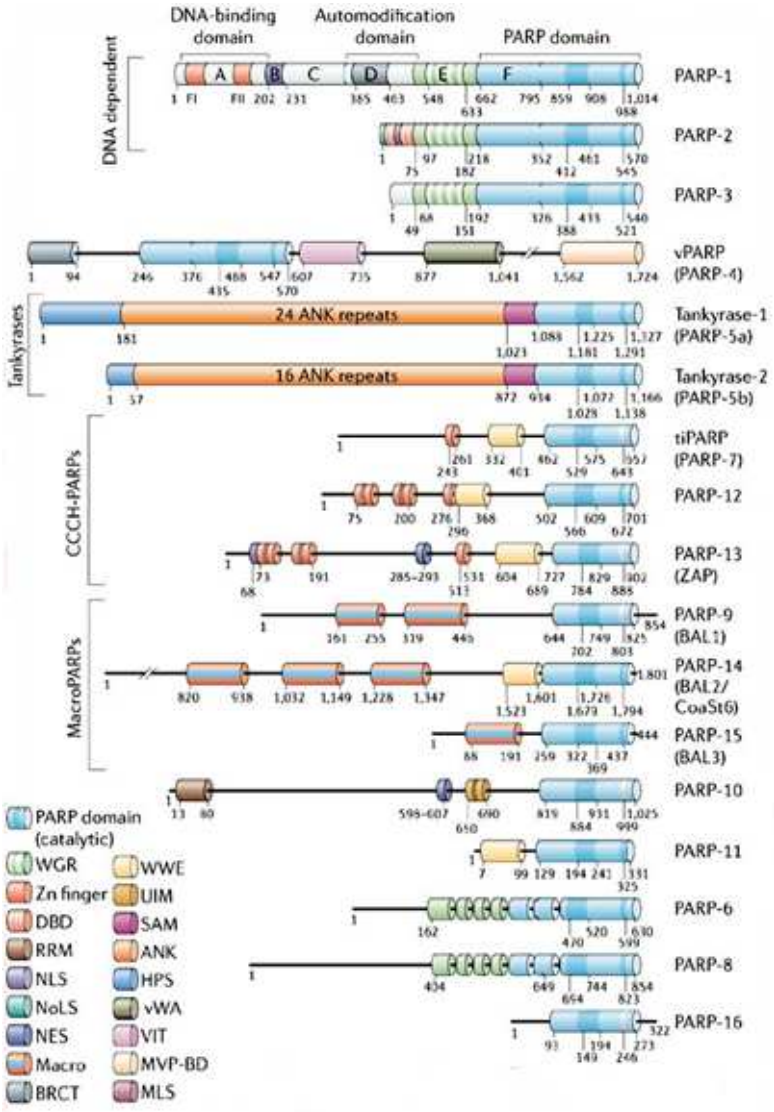

Figure 1. The PARP superfamily. Schematic domain architecture of the 17 members of the PARP superfamily. *Adapted from: Schreiber et al., 2006.*

The PARylation reaction specifically occurs in response to DNA damage. The prototypical enzyme participating in this modification is an abundant nuclear enzyme, poly(ADP-ribose) polymerase-1 (PARP-1). NAD^+ serves as donor of ADP-ribose residues (Miwa and Sugimura, 1984). The synthesis of the polymer requires three PARP activities. First, the initiation or mono-ADP-ribosylation of specific histidine residues, then transfer to a glutamate or aspartate residue(s) in the corresponding PARP enzyme (acceptor), finally the elongation and branching of the polymer (Hassa and Hottiger, 2008) (**Figure 2.**). Polymers can be detected as early as 2 to 3 minutes after the occurrence of DNA damage (Shall, 1984) and the length of those can reach over 200 ADP-ribose units (Miwa and Sugimura, 1984). The half-life of the polymer is very short because of the fast degradation by poly(ADP-ribose) glycohydrolase (PARG) enzyme.

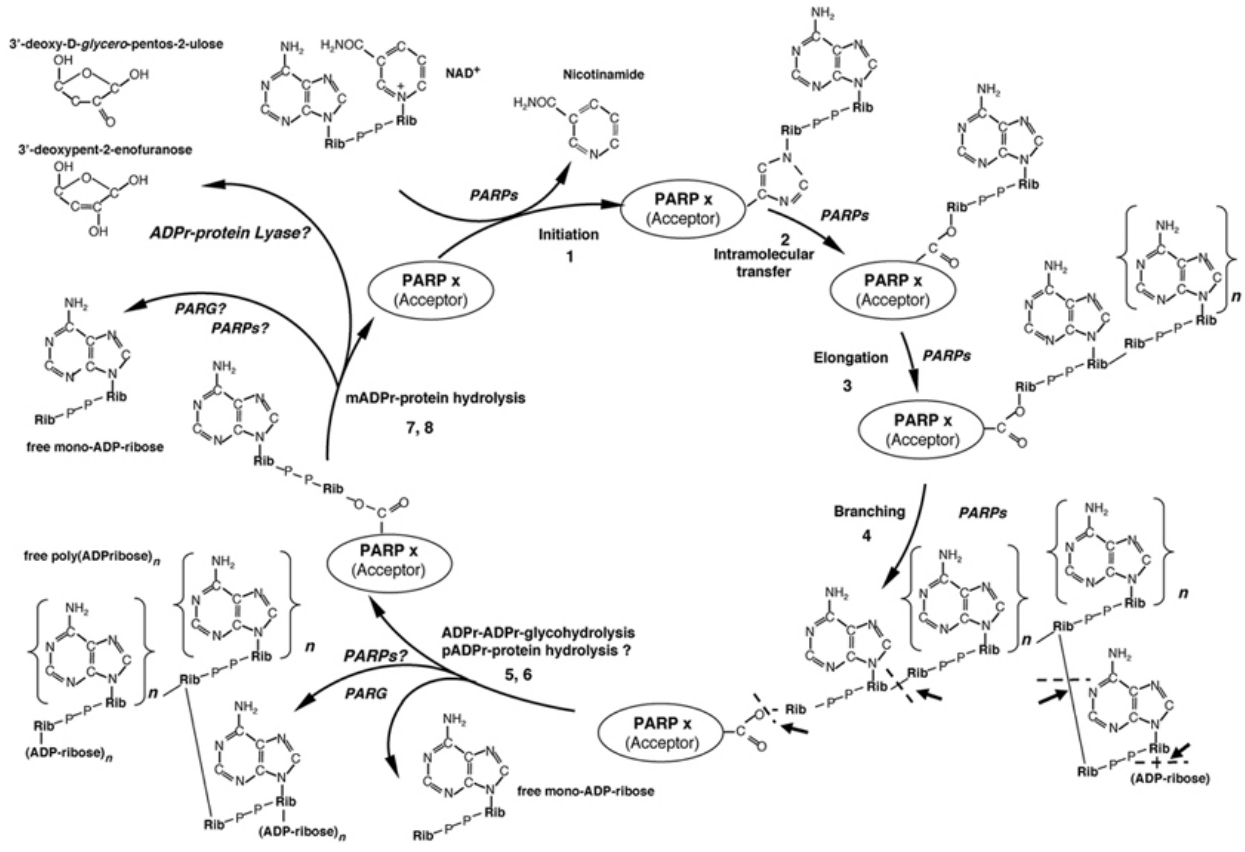

Figure 2. PARylation reaction cycle: steps 1-4 and steps 5-8 of the cycle represent the anabolic and catabolic reactions, respectively, in the metabolism of poly-ADP-ribose. *Adapted from: Hassa and Hottiger, 2008.*

PARylation and PARPs are involved in various cellular processes (Schreiber et al., 2006). PARylation, at any level, is likely to have important effects on the acceptor's properties. In the absence of DNA damage the constitutive polymer levels are usually very low and appear as mono- or oligo(ADP-ribose) (Miwa and Sugimura, 1984). These are different in quality and in metabolism than that of the polymer synthesized in response to DNA strand breaks when the levels of ADP-ribose polymers increase by 10-500-fold (Miwa and Sugimura, 1984). Meanwhile cellular NAD^+ levels are correspondingly reduced (Berger et al., 1985). Both constitutive and activated levels of ADP-ribose chains are dependent on the concentration of NAD^+ in cells (D'Amours et al., 1999). Most of the physiological substrates of PARylation reactions are nuclear proteins that are involved in the metabolism of nucleic acids and in the maintenance of chromatin architecture. The main acceptor of PARylation is PARP itself. PARylation has been demonstrated in all higher eukaryotes and also in most lower eukaryotes.

3.2. PARP-2, another DNA-damage dependent PARP

PARP-2 was discovered after detecting residual DNA-dependent PARP activity in *PARP-1*$^{-/-}$ murine embryotic fibroblasts (MEFs) (Shieh et al., 1998). So far PARP-1 (Ménissier-de Murcia et al., 1989), the founding member of the PARP family, PARP-2 (Amé et al., 1999) and PARP-3 (Rulten et al., 2011; Boehler et al., 2011) are the only enzymes whose catalytic activity is immediately stimulated by DNA strand breaks suggesting that they are all crucial members in the cellular pathway occurring in response to DNA damage. It has been shown on numerous occasions that PARP-2 accounts for 5-15% of total PARP activity in cells depending on the model used (Amé et al., 1999; Shieh et al., 1998).

3.2.1. The structure of the *PARP-2* gene and the PARP-2 protein

PARP-2 gene is located on chromosome 14 in human. The gene is driven by a bidirectional promoter that *PARP-2* shares with RNase P (Amé et al., 2001). Such combination of RNA polymerase II and RNA polymerase III genes seems a structure of rare occurrence. Functional TATA and the DSE/Oct-1 expression control elements were identified in the promoter regulating *PARP-2* expression (Amé et al., 2001). Due to alternative splicing, two isoforms of PARP-2 exist. The longer isoform contains an additional 13 amino acids

sequence on the border between the DNA binding domain and domain E. The sequence of *PARP-2* is highly homologous among mammalian species (**Figure 3**).

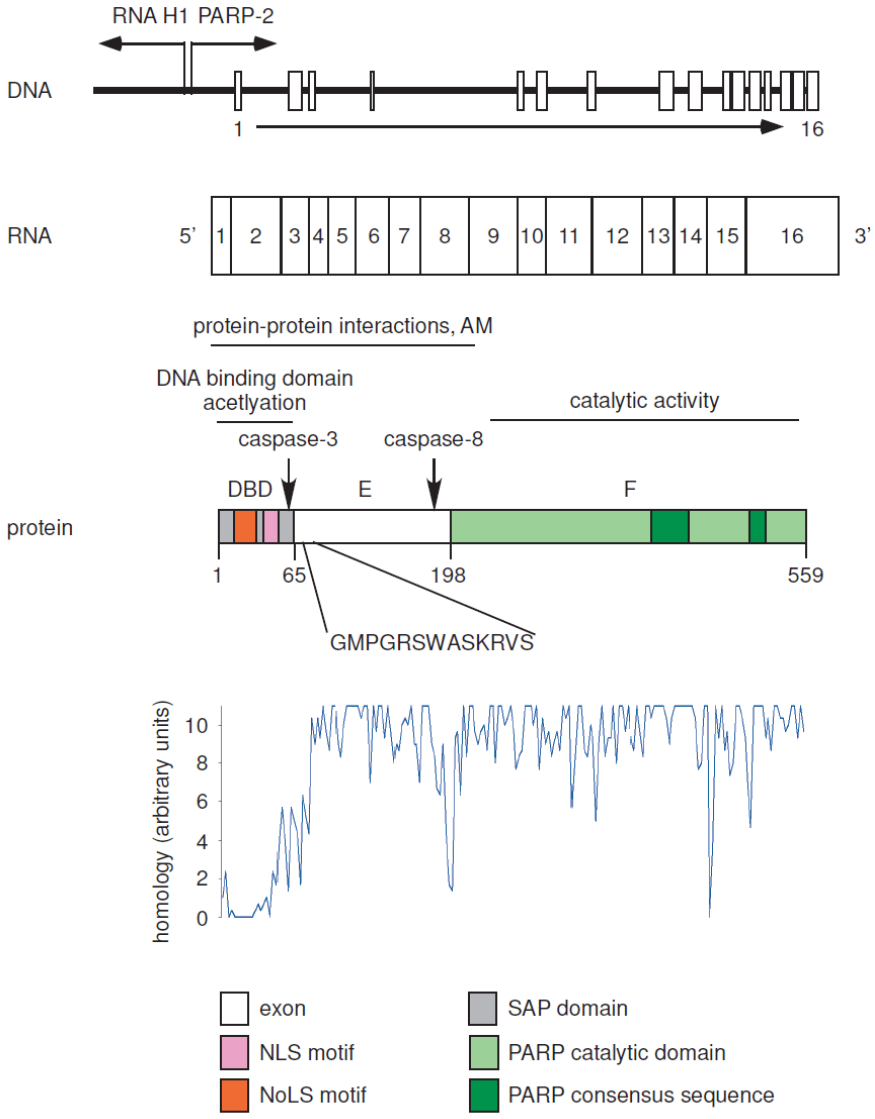

Figure 3. The structure of *PARP-2* gene and PARP-2 protein. The *PARP-2* gene is driven by a bidirectional promoter and consists of 16 exons. The protein product of the gene can be divided into three domains: DBD, domain E, domain F. Numbers below the protein product indicate amino acids on the border between domains. The arrows point at caspases-3 and caspases-8 cleavage sites. The highlighted sequence is the conserved 13 amino acid sequence of the longer PARP-2 isoform.
18 mammalian *PARP-2* sequences of the shorter isoform (*Homo sapiens, Pan troglodytes, Pongo abelii, Nomascus leucogenys, Macaca mulatta, Callithrix jacchus, Mus musculus, Rattus norvegicus, Cricetulus griseus, Cavia porcellus, Monodelphis domestica, Canis lupus familiaris, Bos taurus, Equus caballus, Loxodonta Africana, Sus scrofa, Ailuropoda melanoleuca, Oryctolagus cuniculus*) were compared in the Clustal W2 software (http://www.ebi.ac.uk/Tools/msa/clustalw2/) and relative conservation of the amino acids were plotted. Higher values indicate higher levels of homology.
DBD- DNA binding domain, AM- automodification, NLS- nuclear localization signal, NoLS- nucleolar localization signal, SAP- SAP domain

Although PARP-2 is apparently absent in birds, sequences similar to *PARP-2* can be found in lower vertebrates (Danio rerio, Xenopus), lower animals (e.g. sponges) and in Arabidopsis (Doucet-Chabeaud et al., 2001).

PARP-2 protein (62 kDa) consists of similar functional regions as PARP-1. The N-terminus of mouse PARP-2 contains the DNA binding domain (DBD), followed by domain E and the catalytic domain (domain F) (Amé et al., 1999). The SAP domain inside the DBD is responsible for DNA binding. The DBD also contains a functional nuclear localization signal (NLS) (Haenni et al., 2008) and nucleolar localization signal (NoLS) (Meder et al., 2005). A caspase-3 cleavage site defines the border between the DBD and domain E, which is homologous to the caspase-3 site in the E domain of PARP-1 (Menissier-de Murcia et al., 2003). Domain E predominantly serves as a homodimerization interface, an automodification domain and a protein-protein interaction domain as well (Yelamos et al., 2008). Auto-PARylation of PARP-2 takes place on domain E (Schreiber et al., 2004) and on lysine 36 and 37 that are targets of acetylation simultaneously (Haenni et al., 2008; Altmeyer et al., 2009). Domain F on the C-terminus of PARP-2 contains the PARP signature motif carrying the essential amino acid residues for catalysis (Amé et al., 2009). Domain F is separated from domain E by a caspase-8 cleavage site (Benchoua et al., 2002) (**Figure 3.**).

PARP-2 and PARP-1 share a catalytic domain of 69% similarity, with the exception that PARP-2 contains an additional three amino acids insertion in the loop connecting the β-strands *k* and *l* in PARP-1 (Amé et al., 1999; Oliver et al., 2004; Karlberg et al., 2010). Within this loop there is a side chain which has no equivalent in PARP-1 and points directly into the acceptor site. This specific region presumably acts as a binding site for the elongation of the growing ADP-ribose polymer chain (Schreiber et al., 2004). The three dimensional structure of the catalytic domain equally shows high similarity, however the catalytic domain of PARP-2 has a narrower catalytic cleft that is probably the reason for the lower substrate affinity and turnover rate of PARP-2 compared to PARP-1 (K_M for NAD^+ 50/130 mM; k_{cat}/K_M 6000 s^{-1} M^{-1}/323 s^{-1} M^{-1} for PARP-1/-2 respectively) (Amé et al. 1999; Oliver et al., 2004) (**Figure 4.**).

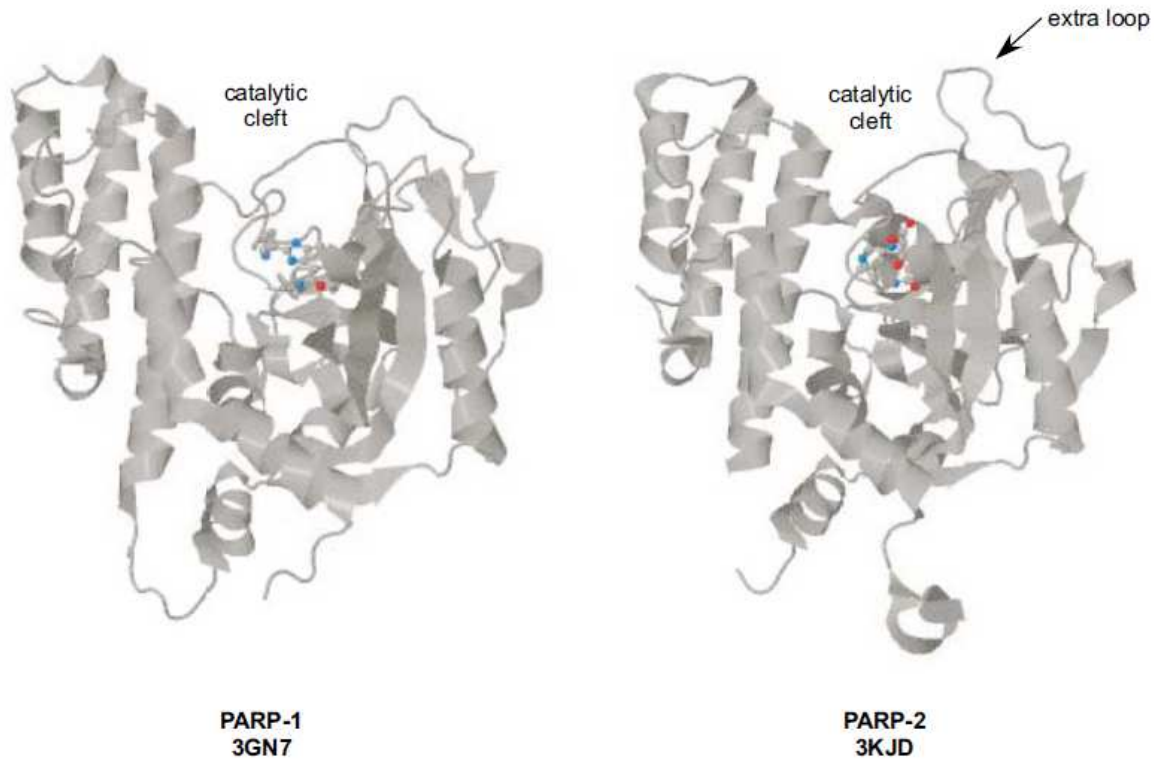

Figure 4. The three dimensional structure of the catalytic domain of PARP-1 and PARP-2. Crystal structure of PARP-1 (3GN7) and PARP-2 (3KJD) were retrieved from the protein data bank (PDB, www.rcsb.com). Both structures contain an inhibitor (in color), the PARP-1 catalytic domain is in complex with A861696, while the PARP-2 catalytic domain is in complex with ABT-888 (Karlberg et al., 2010). The catalytic cleft and the PARP-2 specific loop is indicated.

The observed differences between the catalytic domain of the two enzymes and the fact that PARP-1 and PARP-2 have different targets both in DNA and in chromatin (Yélamos et al., 2008), suggest that they play specific functions in cells.

3.2.2. Expression pattern of *PARP-2*

PARP-2 expression in tissues shows different pattern than that of *PARP-1*, or *PARP-3*. *In situ* hybridization was performed on fetal and newborn mice. In the fetus, *PARP-2* was expressed highly in the thymus. Liver expression of *PARP-2* was high at fetal age 12.5 days that decreased at 18.5 days fetal age and was even lower in newborn mice (Amé et al., 1999; Schreiber et al., 2002). It is tempting to speculate that the gradual decrease in *PARP-2* expression by age suggests that PARP-2 might have a role in early stage haemopoiesis that takes place in the liver.

In the central nervous system PARP-2 content was high in the spinal ganglia and in certain parts of the brain. In the neocortical areas *PARP-2* expression is elevated as compared to lower brain regions. High *PARP-2* expression was detected in stratum granulosum of the dentate gyrus and the stratum pyramidale of the hippocampus and was even higher in the cortex and the olfactory bulb (Schreiber et al., 2002). Apart from the previously mentioned tissues, *PARP-2* is highly expressed in the cortical region of the kidney, and in skeletal muscle, spleen, adrenal gland, stomach, thymus and intestinal epithelium (Schreiber et al., 2002). The testis was also positive for *PARP-2* expression.

In humans slightly different expression pattern was detected. PARP-2 was very abundant in skeletal muscle, brain, heart, testis, high in pancreas, kidney, placenta, ovary, spleen and low PARP-2 expression was detected in lung, leukocytes, gastrointestinal tract (both colon and small intestine), thymus and liver (Johansson, 1999).

3.2.3. The interactome of PARP-2

PARP-2 performs auto- (Schreiber et al., 2002) and hetero-PARylation of proteins. Troiani and co-workers have identified possible targets of PARP-2 activity that covered proteins involved in transcription, translation and mitochondrial organization (Troiani et al., 2011).

The PARP-2 interactome was mapped by Isabelle and co-workers (Isabelle et al., 2010) in an affinity-purification mass spectrometry (AP-MS) analysis that identified 42 interactors of PARP-2. These proteins covered a wide array of functions such as cell cycle, cell death, DNA repair, DNA replication, transcription, metabolism, energy homeostasis and RNA metabolism. Only a part of these proteins interact exclusively with PARP-2, while the others are shared with PARP-1. The authors also carried out a complementary immunoblot analysis to check the affinity purification protocol. This revealed new PARP-2 interactors that were absent from AP-MS, such as BTF (Bcl-2 associated transcription factor), AIF (apoptosis-inducing factor) and STAT1 (signal transducer and activator of transcription 1).

3.3. Specific functions of PARP-2

3.3.1 The role of PARP-2 in the maintenance of genomic integrity

3.3.1.1. PARP-2 in DNA repair and genomic integrity

Several scientific studies have provided evidence for key shared functions of PARP-1 and PARP-2 in the cellular response to DNA damage (Yélamos et al., 2008). The *PARP-2*$^{-/-}$ phenotype in mice involves hypersensitivity to ionizing radiation and alkylating agents (Yélamos et al., 2008). At the cellular level, PARP-2 deficiency leads to chromosomal breaks (Ménissier-de Murcia et al., 2003). PARP-1 and PARP-2 are understood to be the key sensors of DNA-strand breaks which are normally repaired by the SSBR or BER pathways (Schreiber et al., 2006). It is reported that the depletion of PARP-2 in human A549 cells have only little effect on global SSBR (Fisher et al., 2007). However, as shown in murine models, upon the loss of PARP-2 base excision repair (BER) slows down (Schreiber et al., 2002). Moreover, it is reported that PARP-2 interacts with BER factors XRCC1, DNA polymerase β and DNA ligase III, all being PARP-1 partners as well (Schreiber et al., 2002). Taken together, it is tempting to suggest that PARP-2 is an important contributor to the SSBR/BER processes, similarly to PARP-1. This is strengthened by the observation of embryonic lethality of the *PARP-1*$^{-/-}$*PARP-2*$^{-/-}$ double-mutant mice (Ménissier-de Murcia et al., 2003) that might be due to the strong impairment of DNA repair processes. PARP-1 and PARP-2 were shown to accumulate with different kinetics at laser-induced DNA damaged sites, PARP-2 acting with a slower pace (Mortusewicz et al., 2007). It has also been reported that PARP-1 and PARP-2 have different targets both in DNA and in chromatin (Schreiber et al., 2004). Unlike PARP-1 which binds to SSB, PARP-2 has a higher affinity for gaps or flaps, structures that requires more advanced repair intermediates (Yélamos et al., 2008). However, the precise contribution of PARP-2 in SSBR/BER processes needs to be elucidated in future studies.

There are reports in the literature suggesting a role of PARP-2 in double strand break (DSB) repair. Nicolás and co-workers have identified the accumulation of double strand breaks in *PARP-2*$^{-/-}$ murine thymocytes (Nicolás et al., 2010), in line with that Yélamos and colleagues suggested that PARP-2 interacts with the Ku proteins involved in DSB repair (Yélamos et al., 2008). The fact that the double *ATM/PARP-2* knockout genotype is embryonic lethal (Huber et al., 2004) further supports the involvement of PARP-2 in DSB repair during replication. Moreover, mitomycin C treatment that leads to DNA DSB have

provoked the induction of PARP-2 and other DSB repair proteins in human cervical carcinoma cells that further underlines the involvement of PARP-2 in this process (Kang et al., 2010). However it is of note that the exact role of PARP-2 in DSB requires further exploration.

Appropriate telomere and centromere maintenance also requires PARP-2. PARP-2 binds to and negatively regulates the DNA-binding activity of the telomere-binding protein, TRF-2 in different rodent and human cell models. In that way the loss of PARP-2 increased the frequency of spontaneous chromosome and chromatid breaks and of ends lacking detectable telomere repeats (Dantzer et al., 2004).

The occurrence of spontaneous and DNA-damage induced chromosome mis-segregation was observed in *PARP-2*$^{-/-}$ mice and cells. PARP-2 localizes to mammalian centromeres in human and murine cells in a cell-cycle dependent manner and interacts with the kinetochore proteins centromere protein A (CENPA), centromere protein B (CENPB) and mitotic spindle checkpoint protein BUB3 in prometaphase and metaphase (Saxena et al., 2002). Interestingly, this centromeric accumulation of PARP-2 is increased when microtubule dynamics are disrupted (Dantzer et al., 2006).

These observations suggest an essential role of PARP-2 in accurate chromosome segregation through the maintenance of centromeric heterochromatin structure (Dantzer et al., 2006).

3.3.1.2. PARP-2 in chromatin remodeling and genome maintenance during spermiogenesis

PARP-2 is highly expressed in human testis (Johansson, 1999). The expression pattern analysis of *PARP-1* and *PARP-2* in different tissues in mice has shown that it is only in the testis that the expression pattern of the two genes is the most distinct (Schreiber et al., 2002). This, in itself, prompted a study of dissecting the testicular function of PARP-2 (Dantzer et al., 2006). The study showed that PARP-2-deficient mice exhibit severely impaired spermatogenesis due to a defective meiotic prophase I. Though telomere dynamics of the spermatocytes were normal. These features lead to smaller testis size and male hypofertility in *PARP-2*$^{-/-}$ mice.

Probably decreased spermatogenesis has multiple roots that all trace back to insufficient maintenance of genomic integrity during spermatocyte differentiation.

Spermiogenesis involves the compaction of DNA and the change of histones to different protamines (Fuentes-Mascorro et al., 2000). In that process PARP-2 (and PARP-1) regulates the activity of topoisomerase IIβ that is essential for appropriate DNA organization (e.g removal of histone 1) (Meyer-Ficca et al., 2011) transition protein 2 (TP2) and the transition chaperone HSPA2 (Quenet et al., 2009) as shown in mice.

These observations identify PARP-2 as an epigenetic regulator controlling the differentiation process of spermatids into spermatozoa and opens the question whether the dysfunction of this protein might be the possible background behind humans' infertility.

3.3.2. The role of PARP-2 in thymopoesis and inflammatory regulation

The earliest reports on PARP-2 have described high *PARP-2* expression in the subcapsular zone of the thymus where lymphocyte proliferation is the highest. *PARP-2* expression gradually decreases towards the center of the thymus as lymphocytes differentiate and mature (Schreiber et al., 2002; Yélamos et al., 2006). *PARP-2* transcripts were detected in the white pulp of the spleen and the Peyer patches in mice, equally indicative of the involvement of PARP-2 in the proliferation of lymphocytes (Schreiber et al., 2002).

In *PARP-2*$^{-/-}$ mice thymocyte numbers were decreased by half comparing to that of wild type or *PARP-1* $^{-/-}$ mice (Yélamos et al., 2006). The reduced number of thymocytes was associated with decreased $CD4^{+}CD8^{+}$ double-positive (DP) cell survival rather than by a lower cell proliferation rate. The data showed an abnormal regulation of programmed cell death of thymocytes in the absence of PARP-2 since *PARP-2*$^{-/-}$ DP thymocytes were highly susceptible to apoptosis induced by p53-dependent pathways. Increased expression of the pro-apoptotic, bcl-2 homolog NOXA showed correlation with the enhanced apoptosis (Yélamos et al., 2006). When *PARP-2*$^{-/-}$ mice were bred on a *p53*$^{-/-}$ background, spontaneous lymphomas and to a smaller extent other sarcomas developed in the double knockout mice (Nicolás et al., 2010).

PARP-1 inhibition or *PARP-1* deletion has provided widespread protection in most animal models of inflammation (Virág and Szabó, 2002; Peralta-Leal et al., 2009), however it seems that such protection is more limited in *PARP-2*$^{-/-}$ mice. The lack of PARP-2 inhibits astrocyte activation (Phulwani et al., 2008) and provides protection against colitis (Popoff et

al., 2002), while has no effect in models of contact hypersensitivity (Brunyánszki et al., 2010), irritiative dermatitis (Brunyánszki et al., 2010) or pancreatitis (Mota et al., 2005). Interestingly, the lack of PARP-2 suppresses the expression of similar genes as the lack of PARP-1 (*iNOS, IL-1β, TNFα*) (Phulwani et al., 2008; Popoff et al., 2002).

3.3.3. PARP-2 as a regulator of gene expression

PARP-2 acts on multiple levels on gene transcription. Apparently PARP-2 is apt to modify chromatin through regulating transcriptional intermediary factor (TIF) 1β and heterochromatin protein (HP) 1α (Quenet et al., 2008) whereby the depletion of PARP-2 altered the expression of two genes (*Mest* and *HNF4*) dependent on TIF1β-HP1α complex (Quenet et al., 2008). Other studies suggested that PARylation has further roles in epigenetic control (Quenet et al., 2009), which points towards yet uncovered functions of PARP-2.

PARP-2 can also modulate gene expression through direct DNA binding thus influence the expression of different RNA forms. PARP-2 has been shown to interact with nucleophosmin/B23 (Meder et al., 2005) that is involved in rRNA transcription (Derenzini, 2000). Though RNA polymerase I inhibition removes PARP-2 from the nucleolus, the deletion of *PARP-2* does not change rRNA expression. During mRNA expression PARP-2 may act either as a positive co-factor, or a repressor of gene expression. Transcription factors directly regulated by PARP-2 are listed in **Table 1**.

Name	Mode of action	Effects	Model system	Known tissue specificity	Reference
RXR/PPARα	Unknown	Depletion of PARP-2 enhance PPARα activation.	Luciferase reporter system in PARP-2 specific shRNS treated HEK293T cells.	Unknown	Bai et al., 2007.
RXR/PPARδ	Unknown	Depletion of PARP-2 enhance PPARδ activation.	Luciferase reporter system in PARP-2 specific shRNS treated HEK293T cells.	Unknown	Bai et al., 2007.
RXR/PPARγ	Cofactor of receptor	Modulates transcription of PPARγ target genes, Depletion of PARP-2 leads to WAT hypofunction.	Luciferase reporter system in PARP-2 specific shRNS treated HEK293T cells, *PARP-2*$^{-/-}$ mice, *PARP-2*$^{-/-}$ MEFs.	WAT	Bai et al., 2007.
TTF1	Transcriptional cofactor	Regulates the expression of surfactant protein B.	Luciferase reporter system in PARP-2 specific shRNS treated HeLa/MLE15 cells, interaction mapping in mice and in cells.	Lungs	Maeda et al., 2006.

Table 1. Transcription factors directly regulated by PARP-2.

3.3.3.1. Nuclear receptor signaling

PARP-2 is proven to interact with members of the nuclear receptor superfamily, such as peroxisome proliferator activated receptors (PPARs) (Bai et al., 2007).

The class of PPARs have three members (PPARα, PPARδ and PPARγ) (Forman et al., 1996) that heterodimerize with the retinoid X receptor (RXR) and bind to DNA (Fajas et al., 1997; Bardot et al., 1993). PPARs bind different lipophylic ligands (Dreyer et al., 1993) and control the expression of a large number of genes involved in the regulation of energy, lipid and glucose homeostasis (Evans et al., 2004). Binding of ligands leads to receptor activation and the release of corepressor proteins and the subsequent binding of activators (McKenna et al., 2002). PARP-1 has recently been nominated as an interactor in nuclear receptor function. Ju and colleagues have shown that upon estrogen receptor activation topoismerase IIβ creates DNA strand breaks that are resolved through PARP-1 activation. Moreover, inhibition of topoismerase IIβ or PARP-1 impeded efficient gene expression (Ju et al., 2006). Functions of the white adipose tissue (WAT) are orchestrated by the RXR/PPARγ receptor (Fajas et al., 1997). PARP-2 acts as a cofactor for PPARs (Bai et al., 2007). The absence of PARP-2 hampers PPARγ activation, while probably enhances PPARα and PPARδ

activation (Bai et al., 2007). PARP-2 binds to PPARγ-driven promoters and its absence decreases the expression of genes such as *aP2, CD36, LPL, FAS* (Bai et al., 2007). Due to these alterations in gene expression, the WAT of *PARP-2*$^{-/-}$ mice was hypomorphic and hypofunctional (Bai et al., 2007). Similarly to PARP-1, PARP-2 also acts in DNA repair and interacts with topoisomerase IIβ (Meyer-Ficca et al., 2011). Therefore PARP-2 may also take part in resealing transcription-coupled DNA breaks.

3.3.3.2. Thyroid transcription factor-1

Thyroid transcription factor (TTF)-1 belongs to the Nkx-2 family of homeodomain-containing transcription factors. TTF-1 plays a dominant role in lung morphogenesis and respiratory epithelial cell differentiation (Bohinski et al., 1994; Kimura et al., 1996). In cultured lung epithelial cells PARP-2 interacts with TTF1 and thus PARP-2 may regulate the expression of surfactant protein-B (Maeda et al., 2006).

I summarize below the known tissue-specific functios of PARP-2 (**Figure 5.**).

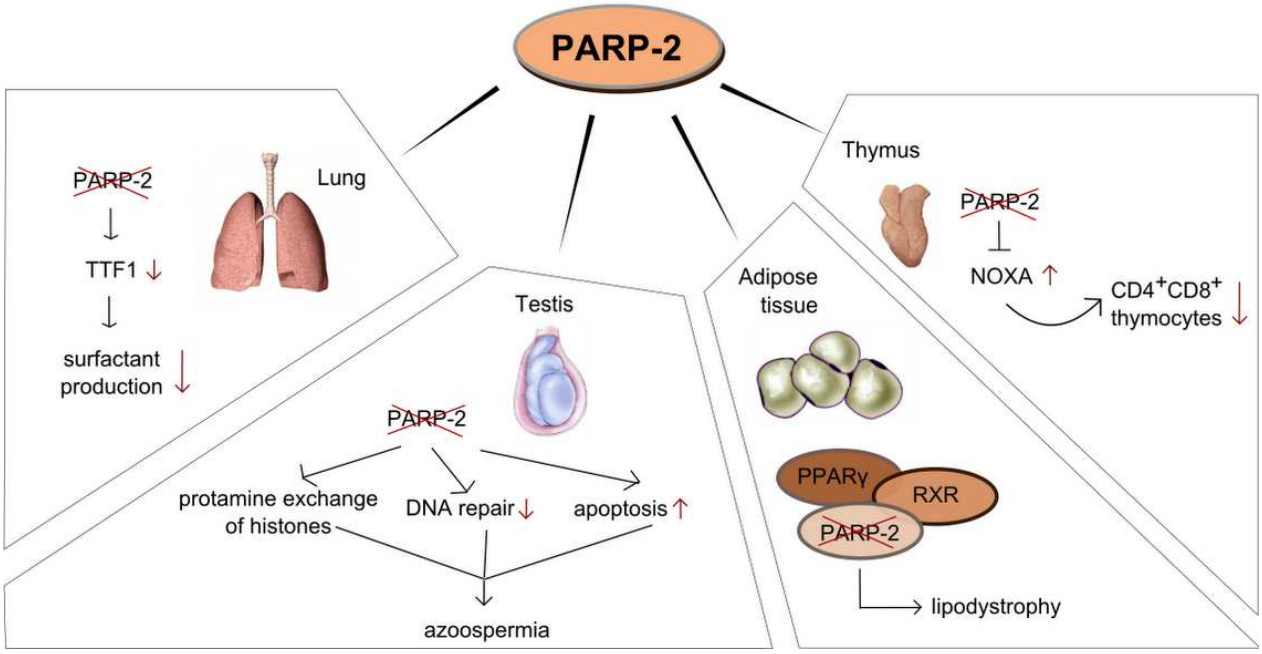

Figure 5. Tissue-specific functions of PARP-2.

3.3.4. The interaction of PARPs with SIRT1 and mitochondrial metabolism

SIRT1 belongs to the family of sirtuins that have seven homologs in human and mice (SIRT1-7) (Blander et al., 2004; Michan et al., 2007). SIRT1 is considered to be a nuclear enzyme (McBurney et al., 2003) although it may also appear in the cytosol (Moynihan et al., 2005). SIRT1 is an NAD^+-dependent protein deacetylase (Imai et al., 2000) (**Figure 6.**).

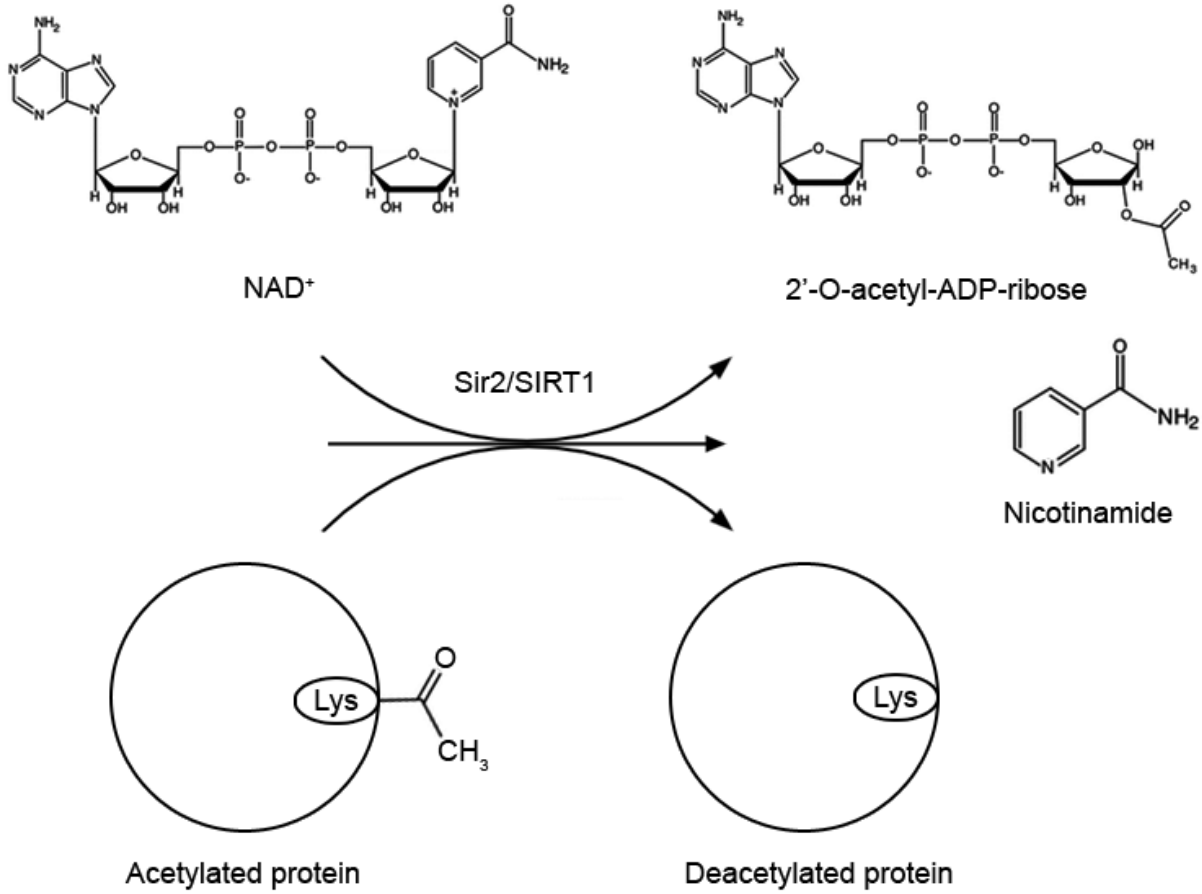

Figure 6. Stochiometry of the deacetylation reaction catalyzed by Sir2/SIRT1. An acetylated protein substrate is deacetylated at the expense of an NAD^+ molecule. On the course of the reaction hydrolysis of NAD^+ and acetyl group transfer to the 2′-OH position of ADP-ribose takes place followed by the formation of 2′-*O*-acetyl-ADP-ribose and nicotinamide.

As for its NAD^+-dependence SIRT1 can act as a sensor of cellular metabolism. Meanwhile its impact on transcription enables SIRT1 to be a regulator of metabolic processes via sensing cellular energy status through NAD^+ availability (Canto and Auwerx, 2011). SIRT1 is activated by increases in NAD^+ levels, or indirectly by different small molecule activators [e.g. resveratrol (Howitz et al., 2003), SIRT1720 (Milne et al., 2007), AMPK activators (Cantó et al., 2009) and PARP-1 inhibitors (Bai et al., 2011[b])]. SIRT1 activation

leads to the deacetylation and activation of numerous metabolic transcription factors such as peroxisome proliferator activated receptor gamma coactivator (PGC)-1α (Rodgers et al., 2005) FOXOs (Brunet et al., 2004). Their activation boosts mitochondrial biogenesis and oxidative metabolism through enhancing the expression of key mitochondrial enzymes involved in mitochondrial respiration, fatty acid oxidation and mitochondrial uncoupling in several target tissues (Rodgers et al., 2005; Lagouge et al., 2006) (**Figure 7.**). SIRT1 induction triggers intense mitochondrial biogenesis by enhancing the expression of *PGC-1α*, *uncoupling protein-2* (*UCP-2*), *acyl coenzyme A oxidase I* (*ACOX1*), *medium-chain specific acyl-CoA dehydrogenase* (*MCAD*), *malonyl-CoA decarboxylase* (*MCD*), *NDufa2*, *Cyt C*, *COXIV* (Bai et al., 2011[b]; Lagouge et al., 2006).

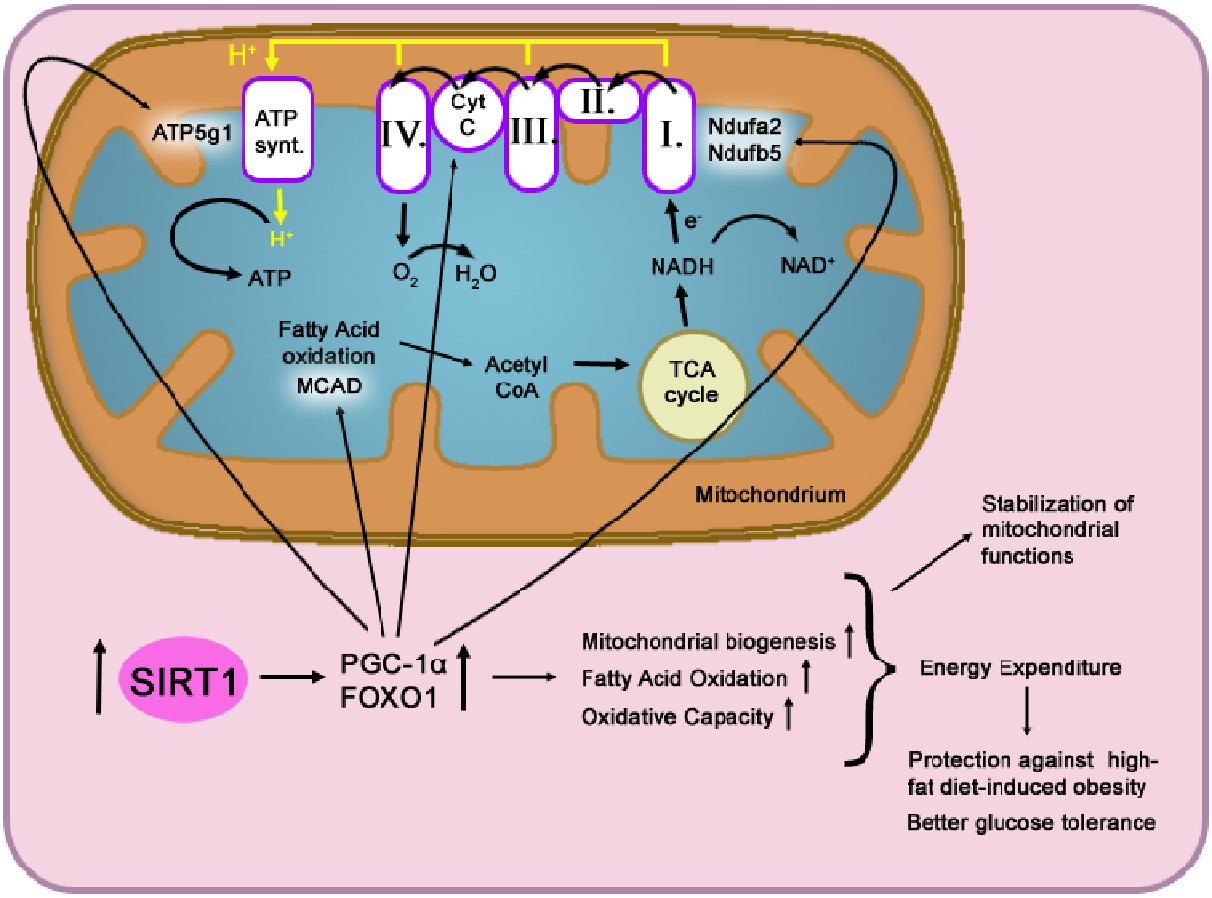

Figure 7. SIRT1 deacetylates and activates PGC-1α and FOXO1 transcription factors, hence boosts mitochondrial biogenesis.

PARP-1 is a major cellular NAD^+ consumer, therefore its activation depletes cellular NAD^+ levels (Sims et al., 1981). It has been shown that in most physiological situations where

NAD^+ levels increased, SIRT1 activity was enhanced (Cantó et al., 2009; Houtkooper et al., 2010; Sauve, 2009). The ability of NAD^+ levels to control SIRT1 activity gave rise to the hypothesis that artificially modulating NAD^+ levels could be effective in the regulation of SIRT1 activity (Houtkooper et al., 2010; Sauve, 2009). One interesting possibility for the artificial modulation of NAD^+ levels relies on the inhibition of alternative NAD^+ consumers, such as CD38 (Young et al., 2006) or PARPs (Bai et al., 2011[b]). Confirming this hypothesis, several laboratories have shown that the activity of PARP-1 and SIRT1 are interrelated due to the competition for the same limiting intracellular NAD^+ pool (Kolthur-Seetharam et al., 2006; Pillai et al., 2005; Bai et al, 2011[b]). PARP-1 activity critically influences NAD^+ bioavailability (Sims et al., 1981), the possible effects of a secondary PARP activity, like PARP-2, on intracellular NAD^+ levels and global metabolism in cells or organs has not yet been fully determined.

3.3.5. PARP-2 in oxidative stress-linked pathologies

PARP-1 is activated upon oxidant-mediated DNA damage. Once activated, it catalyzes the transfer of ADP-ribose moieties from NAD^+ to target proteins. This process depletes intracellular NAD^+ and ATP pools which is a major contributor to cell dysfunction and tissue injury in conditions associated with oxidative stress (Virág and Szabó, 2002; Berger, 1985). It is well understood that the depletion of PARP-1, or its pharmacological inhibition is protective against numerous oxidative stress-related diseases (Virág and Szabó, 2002).

Increased oxidative stress is a major factor implicated in the cardiotoxicity of doxorubicin (DOX) (Pacher et al., 2003). DOX is an anthracycline quinone antitumor drug that has substantial therapeutic activity against a broad variety of human cancers (Davies and Doroshow, 1986). DOX undergoes one-electron reduction to a free radical semiquinone species catalyzed by mitochondria (Davies and Doroshow, 1986). In the presence of molecular oxygen, DOX semiquinone radicals are rapidly reoxidized in a process which generates superoxide, hydroxyl radical or similar reactive oxygen species (Doroshow and Davies, 1986). PARP-1 activation upon free radical evoked DNA-damage and the consequent NAD^+ depletion in the cells contributes to the cardiotoxicity of DOX (Pacher et al., 2002) and provokes cell dysfunction in the vasculature (Murata et al., 2001) (**Figure 8.**).

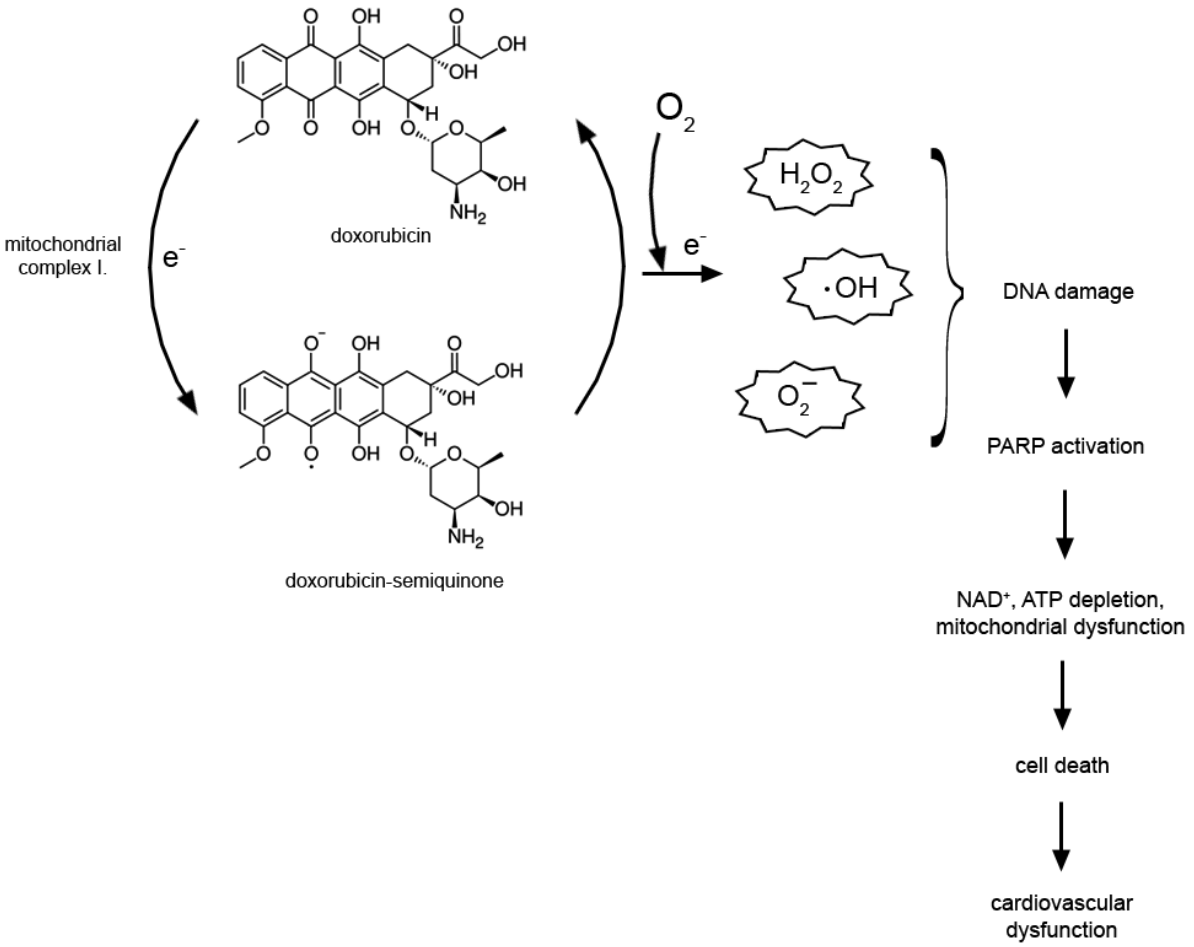

Figure 8. Schematic illustration of the mechanism of DOX-induced cardiovascular dysfunction.

Pillai and colleguages presented a new approach to the mechanism of PARP-1-dependent cardiac cell death during heart failure (Pillai et al., 2005). They have shown that in stressed cardiac myocytes the depletion of cellular NAD^+ levels forms a link between PARP-1 activation and reduced SIRT1 deacetylase activity which contributes to cell death. Reduced SIRT1 deacetylase activity increases the activity of the apoptotic effector p53 (Smith, 2002). It is also of note that PARP-1 is acetylated after stress of cardiomyocytes (Rajamohan et al., 2009). SIRT1 deacetylates PARP-1, which blocks PARP-1 activity and protects cells from PARP-1 – mediated cell death (Rajamohan et al., 2009). PARP-1 activation is also known to cause cell death by translocation of AIF from mitochondria to the nucleus where it induces DNA degradation (Yu et al., 2002). However, it seems to only occur when mitochondrial integrity is compromised (Pillai et al., 2005). Nevertheless, it has been presented that the genetic deletion or pharmacological inhibition of PARP-1 results in protection against DOX-induced heart failure (Pacher et al., 2002; Pacher et al., 2006).

PARP-2 is also known as a PARP activated upon DNA damage (Schreiber et al., 2002). Studies reported that upon the lack of PARP-2 a protective phenotype evolved against injuries caused by diseases linked with increased oxidative stress, such as focal and global cerebral ischemia (Kofler et al., 2006; Li et al., 2010; Moroni et al., 2009), and colitis (Popoff et al., 2002). However, the mechanism by which PARP-2 deletion provides protection is not yet known.

Naturally, knowledge obtained from the research over the role of PARP-1 in oxidative stress-related pathologies can be used as basis for theories. In a model of focal cerebral ischemia ablation of PARP-2 only slightly reduced PAR formation but markedly inhibited the nuclear translocation of AIF (Li et al., 2010), which suggests PARP activation while mitochondrial integrity remained intact. Oxidative stress-related diseases (such as cerebral ischemia, colitis or DOX-induced damage) are associated with mitochondrial damage. SIRT1 activation has been demonstrated to enhance, or restore mitochondrial activity in various tissues (Bai et al., 2011[b]; Lagouge et al., 2006; Danz et al., 2009; Feige et al., 2008; Morris et al., 2011). Moreover, a link between PARP-1 activation and reduced SIRT1 activity has been described in connection with cell death during heart failure (Pillai et al., 2005). These evidence prompted us to study whether the depletion of PARP-2 is protective in DOX-induced tissue injury.

4. LITERARY OVERVIEW AND AIMS OF THE STUDY

SIRT1 has been demonstrated to enhance or restore mitochondrial activity in various tissues (Bai et al., 2011[b]; Lagouge et al., 2006; Danz et al., 2009; Feige et al., 2008; Morris et al., 2011), and reversing mitochondrial damage proved to be successful in counteracting mitochondrial injury caused by oxidative stress-related diseases (Wen et al., 2011; Ye et al., 2011; Hasinoff et al., 2003; Tao et al., 2007; Xu et al., 2002; Panickar et al., 2011), e.g. cerebral ischemia. There are multiple reports that the lack of PARP-2 provides protection against the dysfunction associated with cerebral ischemia (Kofler et al., 2006; Moroni et al., 2009; Li et al., 2010). Moreover, the founding member of the PARP family, PARP-1 was demonstrated to be interconnected with SIRT1 in oxidatively stressed cells (Pillai et al., 2005). These observations prompted us to investigate a possible link between PARP-2 and SIRT1.

On the other hand, it is well known that DOX therapy is also marked by the disruption of mitochondrial membranes (Davies and Doroshow, 1986) causing cardiovascular injury, against which *PARP-1*$^{-/-}$ mice were protected (Pacher et al., 2002). Furthermore, SIRT1 has been shown to act as a cardiovascular protective factor (Danz et al., 2009; Alcendor et al., 2007; Borradaile et al., 2009; Pillai et al., 2005; Rajamohan et al., 2009). These studies furthered the examination of a possible protective role of the deletion of PARP-2 in DOX-induced vascular damage.

Our scientific aims were the following:

1. We aimed to explore if PARP-2 interacts with SIRT1.

2. Furthermore, we investigated whether the lack of PARP-2 is protective in a model of doxorubicin-induced oxidative damage.

5. MATERIALS AND METHODS

5.1. Chemicals

Unless stated otherwise, all chemicals were purchased from Sigma-Aldrich Co. (St. Louis, MO, USA).

5.2. Cell culture

Murine myocytes, C2C12 cells (ECACC cell bank) were cultured in 5% CO_2 atmosphere at 37 ^{o}C in Dulbecco's modified Eagle's medium (DMEM, 4.5 g/l glucose) containing 10% heat-inactivated fetal bovine serum (FBS), 100 U/ml penicillin and 100 µg/ml streptomycin. Cells were differentiated in DMEM (1 g/l glucose) supplemented with 2% horse serum for 2 days and then the cells were considered myotubes. C2C12 cells transduced with lentiviral short hairpin RNA (shRNA) and scrambled (sc) constructs against PARP-2 were then constantly maintained under puromycin selection (2.5 µg/ml).

Murine aortic smooth muscle cells, MOVAS (ATCC cell bank) were maintained in DMEM (4.5 g/l glucose) supplemented with 10% FBS and 0,2 mg/ml G418 (genetycin-GIBCO, Billings, MT, USA) at 37 ^{o}C, 5% CO_2. Transduced MOVAS cells, carrying a scrambled or a PARP-2 shRNA were routinely cultured in the above described media plus 2.5 µg/ml puromycin for maintaining selection of transduced clones.

5.3. Lentiviral infection of C2C12 and MOVAS cells

PARP-2 was depleted in C2C12 and MOVAS cells using lentiviral shRNA system (MISSION Custom Vector). The vectors contained AAG-ATG-ATG-CCC-AGA-GGA-ACT for the interfering PARP-2 sequence and TTC-GGG-GAA-CAA-ACG-TGC-AAC for the control sequence. The transduction of C2C12 and MOVAS cells respectively with control and shPARP-2 lentivirus particles were carried out by the addition of lentivirus into the cell culture with a multiplicity of infection of 20 (20 MOI). Following infection, supernatant was removed after 48 hours and transduced cells were selected with 2.5 µg/ml puromycin for 2×48 hours.

Lowest puromycin concentration that cause 100% cell toxicity (2.5 µg/ml) was previously determined using 3-[4,5-dimethylthiazol-2-yl]-2,5-diphenyl-tetrazolium bromide] (MTT) cell viability assay.

5.4. Animal studies

All animal experiments were carried out according to the national and EU ethical guidelines. Homozygous female *PARP-2*$^{-/-}$ and littermate *PARP-2*$^{+/+}$ on a mixed C57Bl/6J / SV129 (87.5%/12.5%) background from heterozygous crossings were used. Mice were kept under a 12/12 hours dark/light cycle with *ad libitum* access to water and food.

Mice were randomly sorted into 4 groups: *PARP-2*$^{+/+}$ and *PARP-2*$^{-/-}$ control (CTL), and *PARP-2*$^{+/+}$ and *PARP-2*$^{-/-}$ doxorubicin (DOX) (Teva, Debrecen, Hungary) treated. DOX treatment was performed by the administration of 25 mg/kg DOX or saline i.p. Two days post injection mice were sacrificed and aortae were harvested for further experiments.

5.5. Total RNA isolation, reverse transcription and RT-qPCR

Total RNA was prepared applying TRIzol reagent (Invitrogen, Carlsbad, CA, USA) according to manufacturer's instruction. Concentration and quality of RNA was assessed spectrophotometrically using a NanoDrop spectrophotometer (NanoDrop Technologies, Wilmington, DE, USA). 2 µg RNA was used for reverse transcription (RT) with ABI High Capacity cDNA Reverse Transcription Kit (Applied Biosystems, Foster City, CA). Reverse transcription was carried out in a PCR machine using the programme recommended by the manufacturer of the RT kit. Diluted cDNA samples were used for qPCR. All qPCR reactions were performed with Lightcycler 480 II instrument (Roche Applied Sciences, Penzberg, Germany) using Maxima SYBRGreen/ROX qPCR master mix (Fermentas, Glen Burnie, MD, USA). List of primers used is summarized in **Table 2.**

Gene	Primers
ATP5g1	5′-GCT GCT TGA GAG ATG GGT TC-3′ 5′-AGT TGG TGT GGC TGG ATC A-3′
FOXO1	5′-AAG GAT AAG GGC GAC AGC AA-3′ 5′-TCC ACC AAG AAC TCT TTC CA-3′
Ndufa2	5′-GCA CAC ATT TCC CCA CAC TG-3′ 5′-CCC AAC CTG CCC ATT CTG AT-
Ndufb5	5′-CTT CGA ACT TCC TGC TCC TT-3′ 5′-GGC CCT GAA AAG AAC TAC G-3′
Cyt C	5′-TCC ATC AGG GTA TCC TCT CC-3′ 5′-GGA GGC AAG CAT AAG ACT GG-3′
PARP-2	5′-GGA AGG CGA GTG CTA AAT GAA-3′ 5′-AAG GTC TTC ACA GAG TCT CGA TTG-3′
SIRT1	5′-TGT GAA GTT ACT GCA GGA GTG TAA A-3′ 5′-GCA TAG ATA CCG TCT CTT GAT CTG AA-3′
36B4	5′-AGA TTC GGG ATA TGC TGT TGG-3′ 5′-AAA GCC TGG AAG AAG GAG GTC-3′
cyclophyllin	5′-TGG AGA GCA CCA AGA CAG ACA-3′ 5′-TGC CGG AGT CGA CAA TGA T-3′
18S	5′-GGG AGC CTG AGA AAC GGC-3′ 5′-GGG TCG GGA GTG GGT AAT TTT-3′

Table 2. List of primers used in qPCR reactions. All primers refer to murine sequences.

5.6. Mitochondrial DNA (mtDNA) analysis

DNA extraction from cells and from aortae was performed by overnight proteinase K digestion followed by phenol-chloroform extraction. Concentration and quality of DNA was assessed spectrophotometrically. Mitochondrial and genomic DNA was determined in qPCR reactions with a Lightcycler 480 II instrument (Roche Applied Sciences) using Maxima SYBRGreen/ROX qPCR master mix. Specific primers used listed in **Table 3**.

Gene	Primers
mtDNA specific	5′-CCG CAA GGG AAA GAT GAA AGA C- 3′ 5′-TCG TTT GGT TTC GGG GTT TC- 3′
nuclear specific	5′-GCC AGC CTC TCC TGA TTT TAG TGT- 3′ 5′-GGG AAC ACA AAA GAC CTC TTC TGG- 3′

Table 3. List of primers used for mitochondrial DNA measurement. All primers refer to murine sequences.

5.7. Histology and microscopy

Immunohistochemistry was performed on 7 µm paraffin embedded tissue sections or cells with specific antibodies against PAR (1:500), PARP-2 (1:50) (both from Alexis, Lausanne, Switzerland) and smooth muscle actin (SMA) (1:300) (Novocastra, Newcastle upon Tyne, UK) as described in Géhl et al., 2012.

5.8. TUNEL assay

Dewaxed and rehydrated tissue sections or cells attached to coverslips were digested with proteinase K (20 g/ml in 10 mM Tris/HCl pH 7.8) for 30 min at 37 ^{o}C. DNA breakage was labelled with terminal deoxyribonucleotidyl transferase (TdT) and a deoxyribonucleotide mix containing digoxigenin labelled dUTP for 60 min at 37 ^{o}C. Samples were washed with PBS then were incubated with anti-digoxigenin peroxidase conjugated antibody for 30 min at room temperature. Peroxidase was detected by diamino-benzamide reaction. Samples were counterstained with methyl green.

5.9. Malondialdehyde assay

Determination of lipid peroxidation and oxidative stress in tissues was carried out by analyzing malondialdehyde formation measured as thiobarbituric acid-reactive components. Tissues were homogenized in 1.15% KCl buffer. 200 µl of homogenates were added to a reaction buffer consisting of 1.5 ml of 0.8% thiobarbituric acid, 200 µl of 8.1% SDS, 1.5 ml of 20% acetic acid (pH 3.5) and 600 µl of distilled H_2O. The mixtures were incubated for 45 min at 90 ^{o}C then were cooled to room temperature and cleared by centrifugation (10000 × g, 10

min). Supernatant was removed and absorbance at 532 nm was measured in a Labsystem Multiskan MS plate reader (Analytical Instruments, Minneapolis, MN, USA). Results were normalized to protein content. The level of lipid peroxides was expressed as percentage of control.

5.10. Measurement of PARP activity

PARP activity in cell lysates was determined by using the assay based on the incorporation of isotope from ^{3}H-NAD^{+} into TCA precipitable proteins, as described in (Bai et al., 2001) with minor modifications. Cells were seeded in 6-well plates. Cells were induced with 3 µM DOX for 7 hours. H_2O_2 treatment was used as positive control (10 min, 1 mM). Cells were scraped and incubated at 37 ^{o}C in 1.0 ml assay buffer (56 mM HEPES pH 7.5, 28 mM NaCl, 2mM $MgCl_2$, 0.01% digitonin, 0.125 µM NAD^{+} and 0.5 µCi/ml ^{3}H-NAD^{+}). Next, 400 µl ice-cold 50% TCA was added and samples were incubated for another 4 h at 4^{o}C. Then the samples were centrifuged (10000 × g, 10 min) and pellets were washed twice with ice-cold 5% TCA and solubilized overnight in 250 µl 2% SDS/0.1 N NaOH at 37 ^{o}C. Contents of tubes were added to 5.0 ml ScintiSafe Plus scintillation liquid (Fisher Scientific, Pittsburgh, PA, USA) and radioactivity was determined using a liquid scintillation counter (TriCarb2800TR, PerkinElmer, Waltham, MA, USA).

5.11. Oxygen consumption

Oxygen consumption of cells was measured by the application of an XF96 oxymeter (Seahorse Biosciences, North Billerica, MA, USA). Cells were seeded in 96-well assay plates. Following the determination of baseline oxygen consumption, cells received a single bolus dose of DOX (0.3 – 30 µM final concentration) then oxygen consumption was recorded in every 30 minutes. Final reading took place at 7 hours post DOX treatment. Oxygen consumption rate data were normalized to protein content.

5.12. Intracellular NAD^{+} measurement

Cells were seeded in 6-well plates a day before the experiment. Following 7 hours DOX treatment, cells were extracted in 0.5 N $HClO_4$ solution, neutralized with 3 M KOH and

centrifuged at 10000 rpm for 5 min. Supernatants were added to a reaction mixture containing 0.1 mM MTT, 0.9 mM phenazine methosulphate (PMS), 13 U/ml alcohol dehydrogenase, 100 mM nicotinamide and 5.7% ethanol in 61 mM glycil-glycin buffer (pH 7.4). The NAD^+ content of cells was measured photometrically at 560 nm after the enzymatic reaction that is based upon an alcohol dehydrogenase cycling reaction in which the tetrazolium dye is reduced by NADH in the presence of PMS. NAD^+ levels were calculated using a standard curve generated from NAD^+ solutions of known concentration. Data were normalized to protein content.

5.13. Luciferase reporter assay

Cells were seeded in 6-well plates. Transfection took place after cells reached approximately 60% confluency. The transfection mixture contained 8 µg of the corresponding SIRT1 promoter construct (Nemoto et al., 2004) and 4 µg β-galactosidase expression plasmid per 9 µl JetPEI transfection reagent in 200 µl/well 150 mM NaCl solution. 48 hours post-transfection cells were scraped in a lysis buffer (25 mM Tris-phosphate pH 7.8, 2 mM EDTA, 1 mM DTT, 10% glycerol, 1% Triton-X 100) and lysates were divided into two pieces for the determination of luciferase and β-galactosidase activity. Luciferase activity was measured in a Victor luminometer (PerkinElmer) in a media consisting of 20 mM Tris-phosphate pH 7.8, 1.07 mM $MgCl_2$, 2.7 mM $MgSO_4$, 0,1 mM EDTA, 33.3 mM DTT and 270 µM coenzyme A, 470 µM luciferine and 530 µM ATP were added. β-galactosidase activity was measured photometrically at 405 nm in a media containing 0.06 M Na_2HPO_4, 0.04 M NaH_2PO_4, 0.01 M KCl, 1 mM $MgSO_4$, 50 mM β-mercapto-ethanol and substrate ONPG was added. Luciferase activity was expressed as measured luciferase activity/β-galactosidase activity.

5.14. Determination of mitochondrial membrane potential

Mitochondrial membrane potential was analyzed by TMRE (tetramethylrhodamine ethyl ester) staining. Cells were seeded in 96-well plate (25000 cells/well) and treated with DOX (0.3-30 µM, 7 hours). After treatment cells were stained with 25 nM TMRE for 30 min then were washed with Hank's balanced salt solution (HBSS) (0.138 M NaCl, 5.33 mM KCl, 0.338 mM Na_2HPO_4, 0.441 mM KH_2PO_4, 1.26 mM $CaCl_2$, 0.493 mM $MgCl_2$, 0.407 mM $MgSO_4$,

4.17 mM $NaHCO_3$). Fluorescence was measured on 530 nm as excitation and 590 nm as emission wavelengths. TMRE fluorescence was normalized to protein content.

5.15. Determination of superoxide production

Superoxide production was measured by hydroethidine (HE) fluorescent staining. Cells were induced by DOX (3 μM, 7 hours) and were stained with 2 μM HE for 30 min. Then cells were washed, trypsinized and fluorescence was analyzed by flow cytometry (FACSCalibur, BD Biosciences, San Jose, CA, USA). Superoxide production was indicated as a mean of HE fluorescence in each sample.

5.16. Protein extraction and Western blot analysis

Cells in culture dishes were washed with phosphate-buffered saline (PBS) then scraped and pelleted by centrifugation (1500 rpm, 3 min). Cells were homogenized with 5 volume RIPA lysis buffer [1% Nonidet P-40, 1% sodium-deoxycholate, 0.1 % SDS, 0.15 M NaCl, 0.01 M sodium phosphate, 2 mM EDTA, 50 mM sodium fluoride and freshly added 1 mM DTT and protease inhibitor cocktail (1:100)]. Cells were left on ice in lysis buffer for several minutes and vortexed frequently. Then the lysates were homogenized with a 22-gauge needle by drawing up and pushing out for at least 15-times. Lysates were cleared by centrifugation (10000 rpm, 10 min). Protein concentration was determined by BCA protein assay, 50 μg from each extract were separated by SDS-PAGE and were transferred to nitrocellulose membranes. For immunoblotting, membranes were blocked with 5% non-fat dry milk in Tris-buffered saline containing 0.05% Tween20 (TBSTw) for 60 min. Primary antibodies in 1% non-fat dry milk/TBSTw in the following dilutions: SIRT1 (1:1000, Millipore-Upstate, Billerica, MA, USA), PARP-2 (1:1000, Alexis), β-actin (1:1000) were then applied overnight at 4 ^{o}C, respectively. After thorough washing three times with TBSTw, secondary antibodies [peroxidase-conjugated goat anti-mouse or anti-rabbit IgG (both from Sigma)] were applied in 1:5000 dilutions in 1% non-fat dry milk/TBSTw for 1 hour at room temperature. Membranes were washed again three times with TBSTw plus an extra washing with TBS.

To detect antibody binding, Supersignal WestPico Enhanced Chemiluminescence (ECL) substrate (Pierce Biotechnologie Inc., Rockford IL) was applied on membranes.

Photographic film (GE Healthcare, Waukesha, WI, USA) was exposed to chemiluminescence and was developed in a developing machine (Kodak, Rochester, NY, USA).

5.17. Chromatin immunoprecipitation (ChIP)

To fix chromatin-bound proteins on DNA, 1% formaldehyde solution was added on cells in Petri dish for 10 min at room temperature. Cells were washed with PBS then scraped and pelleted by centrifugation (1500 rpm, 3 min) in Eppendorf tubes. Pellets were resuspended in a lysis buffer containing 5 mM piperazine-N,N'-bis(2-ethanesulfonic acid) [PIPES (pH 8)], 85 mM KCl, 0.5% NP-40, and freshly added 1 mM DTT and protease inhibitor cocktail. After centrifugation at 3000 × g for 10 min at 4 ^{o}C, nuclei were resuspended in sonication buffer (1% SDS, 0.1 M $NaHCO_3$, 1 mM DTT and protease inhibitor cocktail), incubated on ice for 10 min and sonicated. Chromatin was cleared by centrifugation at 10000×g for 30 min at 4 ^{o}C. Aliquots of the soluble chromatin was diluted in immunoprecipitation (IP) buffer [1.1% Triton X-100, 1.2 mM EDTA, 16.7 mM Tris (pH 8.1), 16.7 mM NaCl, 1 mM DTT and protease inhibitor cocktail]. Small volume of the chromatin prepared was put aside as input.

Immunoprecipitation was carried out with antibodies against PARP-2 and matrix metalloproteinase-2 (MMP2) by overnight incubation at 4 ^{o}C. We also used a „no antibody" control. Immunoprecipitates were collected with blocked protein A+G sepharose beads (GE Healthcare) by another 4 hours incubation at 4 ^{o}C. Beads then were washed twice with the following buffers respectively: buffer A (low salt) (0.1% SDS, 1% Triton X-100, 2 mM EDTA, 20 mM Tris, pH 8.1, 150 mM NaCl, 1 mM DTT and protease inhibitor cocktail), buffer B (high salt) (0.1% SDS, 1% Triton X-100, 2 mM EDTA, 20 mM Tris, pH 8.1, 500 mM NaCl, 1 mM DTT and protease inhibitor cocktail), buffer C (0.25 M LiCl, 1% NP-40, 1% sodium deoxycholate, 1 mM EDTA, 10 mM Tris (pH 8.1), 1 mM DTT and protease inhibitor cocktail), and TE buffer (10 mM Tris, 10 mM EDTA, pH 8). Cross-links were reversed by overnight incubation at 65 °C under treatment with RNase A (1 µg). Then the beads were treated with 0.5% SDS and 2 µg proteinase K and incubated for 2 hours at 45 °C. Samples were purified by QIAquick PCR purification kit (Qiagen, Valencia, CA, USA). Purified DNA was analyzed by qPCR using the following primers:

SIRT1 -91 FWD: 5'-TCC CGC AGC CGA GCC GCG GGG-3'

SIRT1 -91 REV: 5’-TCT TCC AAC TGC CTC TCT GGC CCT CCG-3’

The results were expressed as a percentage of input.

5.18. Statistical analysis

To determine statistical difference between different groups Student’s t-test was applied and $p<0.05$ was considered significant. Error bars represent ±SEM unless stated otherwise.

6. RESULTS

6.1. PARP-2 regulates oxidative metabolism by repressing the SIRT1 promoter

In order to shed light on the potential role of PARP-2 in the regulation of SIRT1 activity, we generated C2C12 myocytes stably transfected with either a scrambled (sc) or a PARP-2 shRNA. PARP-2 mRNA and protein content is reduced by 60% in myotubes from cells carrying the PARP-2 shRNA (**Figure 9A**.).

We next examined whether this decrease in PARP-2 activity affects NAD^+ homeostasis. The reduction in PARP-2 activity did not significantly affect total NAD^+ levels (**Figure 9B.**) suggesting that PARP-2 inactivation does not affect NAD^+ homeostasis, probably because PARP-2 is a secondary PARP activity in the cell (Amé et al., 1999; Shieh et al., 1998).

Next we analyzed SIRT1 mRNA levels and it proved to be significantly higher in the PARP-2 depleted cells (**Figure 9C.**), and this increase was linked to increased SIRT1 content (**Figure 9C.**). Higher SIRT1 level consequently induced the expression of genes related to lipid and mitochondrial metabolism, such as *medium chain acyl coenzyme A dehydrogenase (MCAD), NADH dehydrogenase (Ubiquinone) 1 alpha subcomplex subunit 2 (Ndufa2), and cytochrome C (Cyt C)* (**Figure 9D.**)

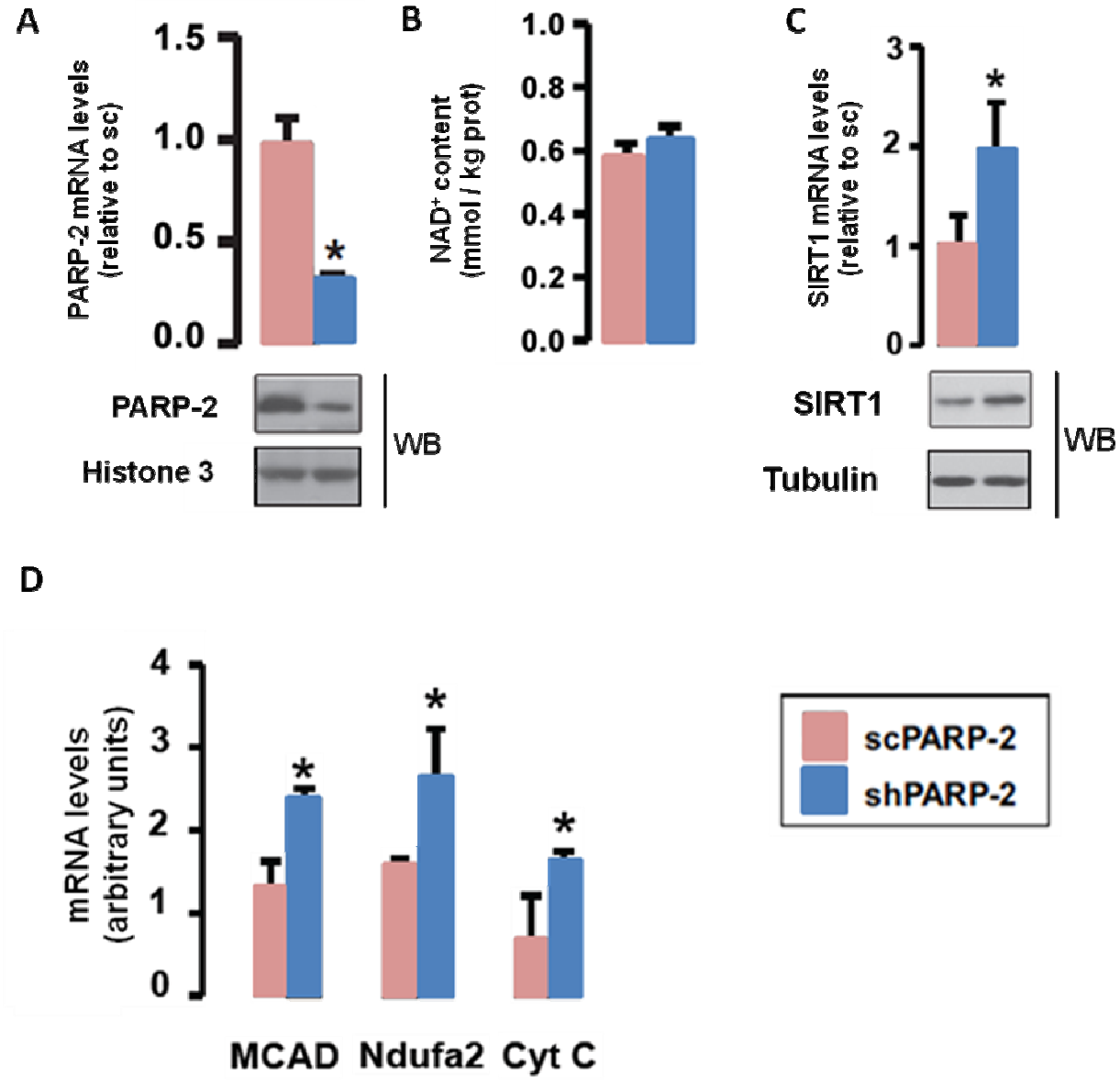

Figure 9. PARP-2 regulates SIRT1 expression and oxidative metabolism. (A) PARP-2 protein and mRNA levels were analyzed in C2C12 myotubes carrying a stably transfected scrambled or PARP-2 shRNA. **(B)** NAD^+ content was evaluated in C2C12 myotubes stably transfected with a scrambled or a PARP-2 shRNA. **(C)** SIRT1 mRNA levels and protein content were analyzed in C2C12 myotubes carrying a stable transfection with either scrambled or PARP-2 shRNA (WB: Western blot). **(D)** mRNA levels of the markers indicated were measured in C2C12 myotubes carrying a stable transfection with either a scrambled or a PARP-2 shRNA. All results are expressed as mean ± SD. * indicates statistical difference versus scPARP-2 cells at $p<0.05$.

To find an explanation to these phenomena we performed ChIP assay where PARP-2 was shown to bind directly to the proximal SIRT1 promoter (region between the transcription start site and -91 bp) in C2C12 cells (**Figure 10A.**). In luciferase reporter assays we used reporter constructs in which serial deletions of the mouse SIRT1 promoter controlled luciferase expression (**Figure 10B.**). The results demonstrated that knocking down

PARP-2 promoted a 2-fold increase in SIRT1 promoter activity through the very proximal promoter region (-91 bp), as the shortest construct already showed the enhancement of SIRT1 promoter activity upon PARP-2 depletion (**Figure 10B.**). These data let us conclude that PARP-2 acts as a direct negative regulator of the SIRT1 promoter, as reduction in PARP-2 levels induced SIRT1 transcription, leading to higher SIRT1 protein levels and SIRT1 activity.

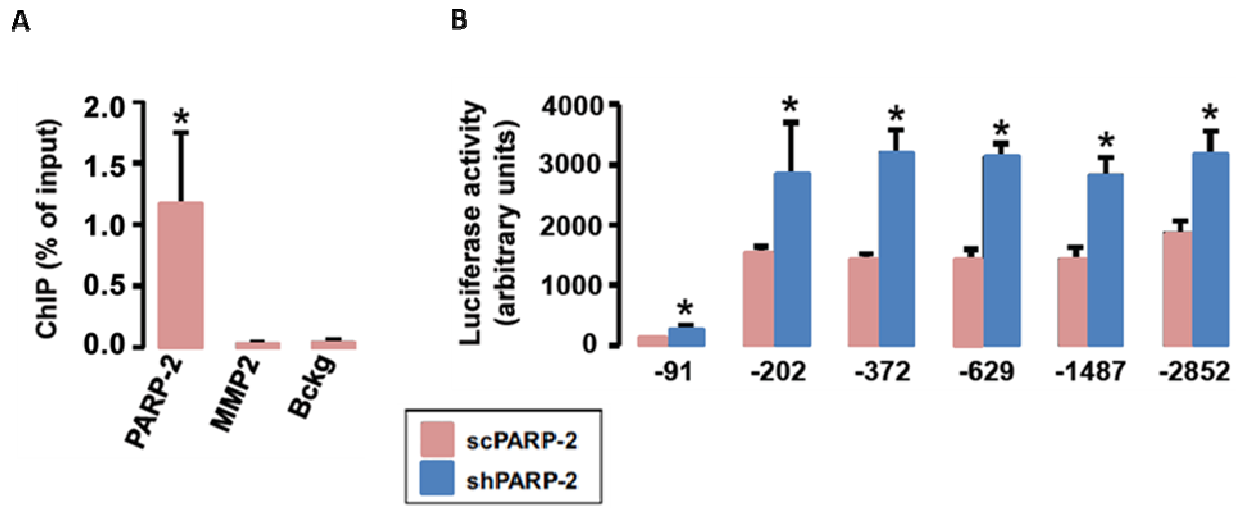

Figure 10. PARP-2 acts as negative regulator of the SIRT1 promoter. (A) The presence of PARP-2 on SIRT1 (-1 through -91) promoter was assessed in C2C12 cells by ChIP assays, using MMP2 as negative control. Bckg refers to background, "no antibody" control. **(B)** The activity of nested deletions of the SIRT1 promoter was measured in C2C12 cells carrying a stable transfection with either a scrambled or a PARP-2 shRNA. All results are expressed as mean ± SD. * indicates statistical difference versus scPARP-2 cells at $p<0.05$.

6.2. The role of PARP-2 in doxorubicin (DOX)-induced vascular damage

6.2.1. Effects of PARP-2 depletion on aortic smooth muscle after DOX-treatment

Characterization of the vascular functions of *PARP-2*$^{+/+}$ and *PARP-2*$^{-/-}$ mice after DOX-treatment suggested a role for PARP-2 in DOX-evoked vascular dysfunction since DOX treatment significantly decreased the aortic contractile force of *PARP-2*$^{+/+}$ mice, while deletion of *PARP-2* was partially protective (data not shown). In line with that hypothesis, after DOX-treatment smooth muscle actin (SMA) immunoreactivity decreased in *PARP-2*$^{+/+}$ mice, while it was retained in *PARP-2*$^{-/-}$ mice (**Figure 11.**), suggesting conservation of smooth muscle cells.

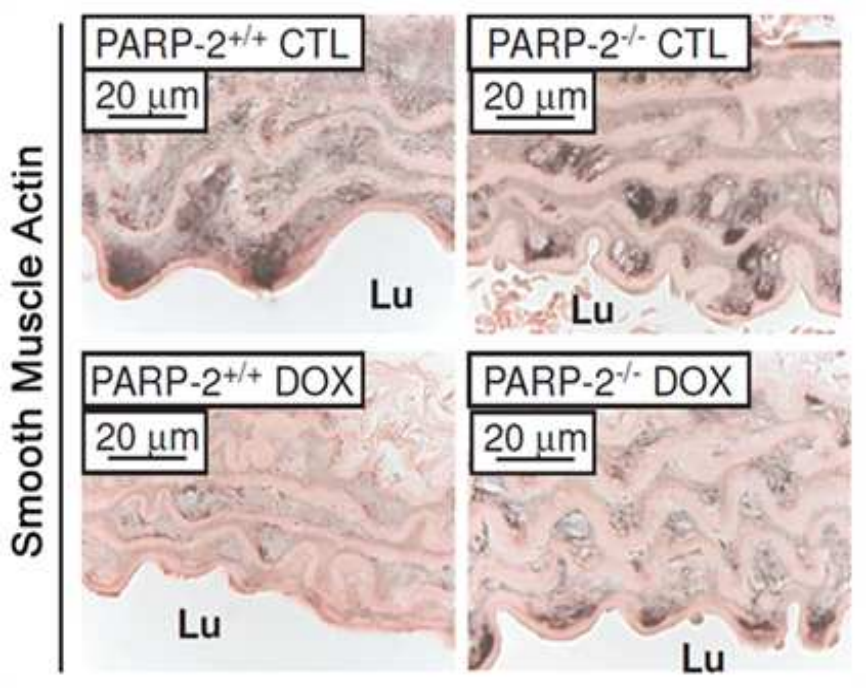

Figure 11. Genetic deletion of PARP-2 protects against DOX-induced aortic smooth muscle damage. SMA immunoreactivity decreased in *PARP-2*$^{+/+}$ mice after DOX treatment, suggesting a loss of smooth muscle cells, which was not the case in *PARP-2*$^{-/-}$ mice. Luminal side is indicated (Lu), scale bar is 20 µm.

To study aortic smooth muscle function, in our following experiments we introduced an aortic smooth muscle cell line (MOVAS) to unveil the potential mechanisms of PARP-2 involvement in DOX-evoked vascular dysfunction.

6.2.2. DOX-induced PARP activation is not affected by PARP-2 depletion

We set out to investigate the role of PARP-2 in DOX-evoked PAR synthesis. We detected free radical production upon DOX treatment in aortae derived from *PARP-2*$^{+/+}$ and $^{-/-}$ mice and in MOVAS cells (control and shPARP-2) as well. This occurred independently of the deletion of PARP-2. Moreover, free radical production increased upon PARP-2 ablation (**Figures 12A and 13A.**). Enhanced free radical production resulted in DNA strand breakage in both types of samples as judged by increased TUNEL staining, and was again independent of the genotype (**Figures 12B and 13B.**).

PARP-2 ablation did not alter DOX-induced PARP activation (**Figure 12C.**) in the aortae of *PARP-2*$^{+/+}$ and $^{-/-}$ mice. Similarly, there was no difference in PARP activation (**Figure 13C.**), nor in the consequent NAD^+ depletion (**Figure 13D.**) in MOVAS cells in which PARP-2 was silenced by specific shRNA or in those carrying its unspecific scrambled version. These

results suggested a dominant role for PARP-1 in DOX-evoked PAR formation. However, PAR was detected only in smooth mucle cells in aortae suggesting that the DOX-evoked endothelial dysfunction of the vasculature is PARP-independent, at least 2-days post-treatment. Taken together, PARP-2 depletion or deletion protects vascular smooth muscle against DOX-induced damage without affecting DOX-induced overall PARP activity.

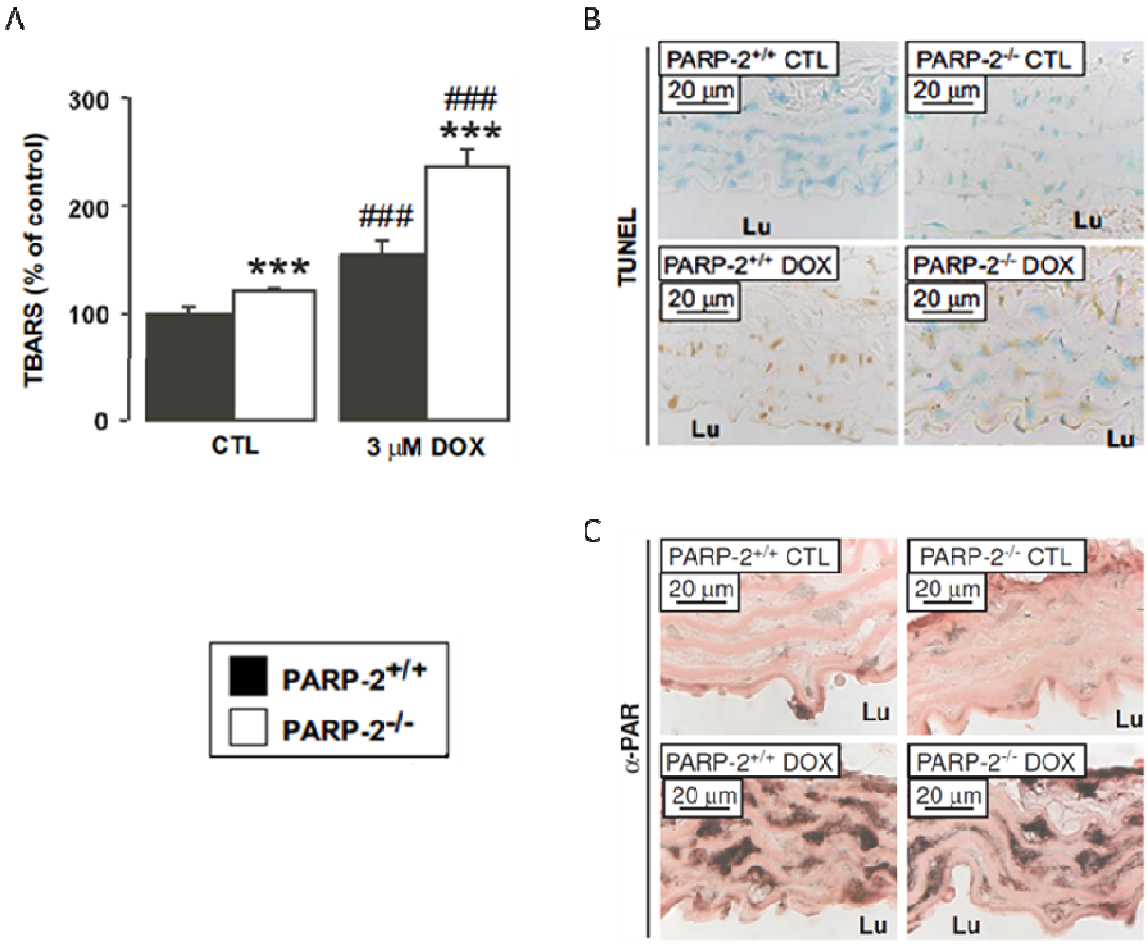

Figure 12. Deletion of PARP-2 does not affect free radical-induced PARP activation in aortae of mice. *PARP-2*$^{+/+}$ and *PARP-2*$^{-/-}$ mice were injected with saline (CTL) or with 25 mg/kg DOX at 3 months of age (n=5 for *PARP-2*$^{+/+}$ CTL, n=5 for *PARP-2*$^{-/-}$ CTL, n=5 for *PARP-2*$^{+/+}$ DOX, and n=4 for *PARP-2*$^{-/-}$ DOX). Measurements were performed 2-days post-DOX injection. **(A)** Free radical formation was measured by determining thiobarbituric acid reactive species. **(B)** DNA breaks were detected using TUNEL assay; scale bar represents 20 µm. **(C)** PAR formation in paraffin-embedded aortae was assessed with an anti-PAR antibody; scale bar represents 20 µm. Lu, lumen; ### indicate statistically significant difference between CTL and DOX-treated groups, at P<0.001, *** indicate statistically significant difference between *PARP-2*$^{+/+}$ mice and *PARP-2*$^{-/-}$ mice at P <0.001.

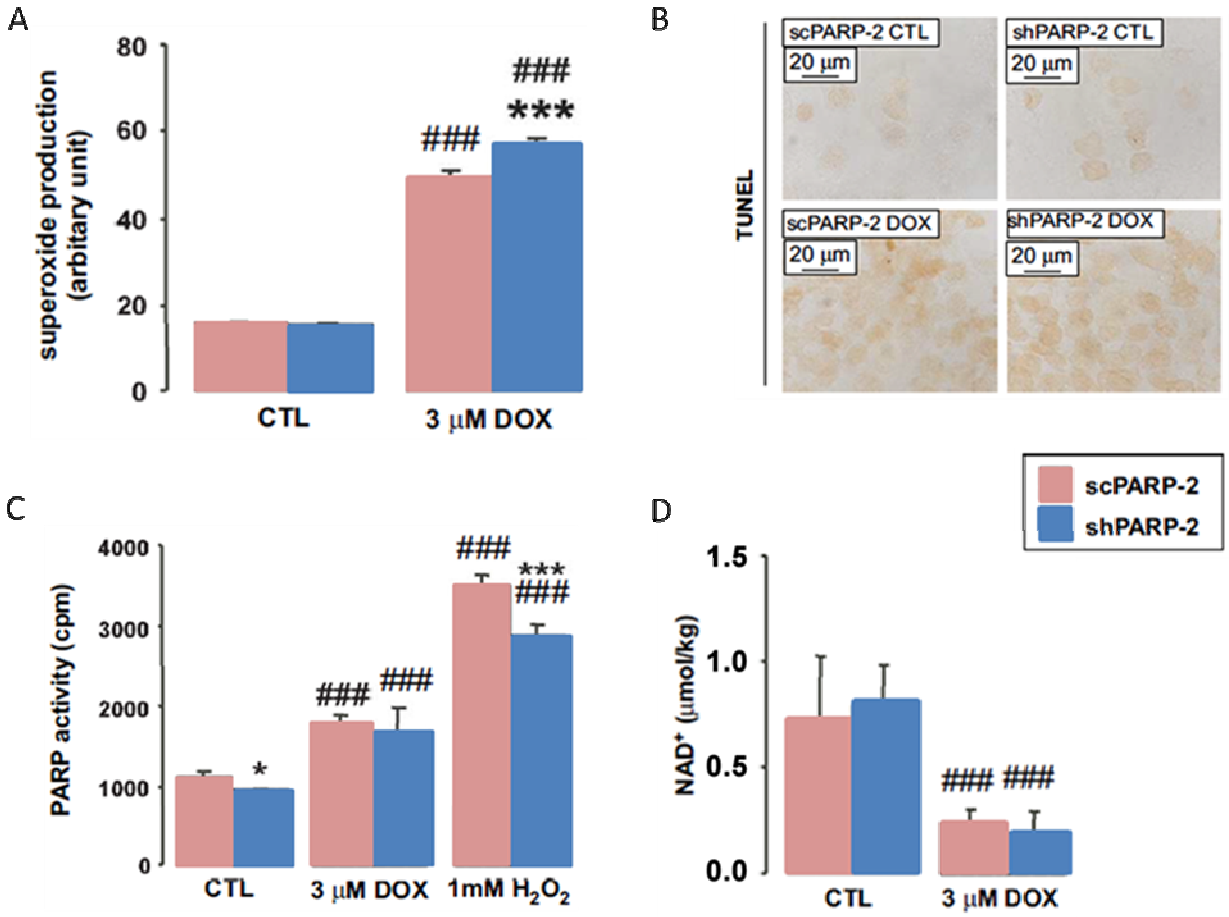

Figure 13. Deletion of PARP-2 does not affect free radical-induced PARP activation or NAD^+ depletion in cultured aortic smooth muscle cells. An aortic smooth muscle cell line (MOVAS) was also tested (n=3 parallel measurements). MOVAS cells were transduced with a PARP-2-silencing (shPARP-2) or -scrambled (scPARP-2) shRNA and treated with solvent (CTL), 3 µM DOX or with 1 mM H_2O_2. Measurements were performed 7 h after DOX treatment. **(A)** Free radical formation was measured by HE fluorescence. **(B)** DNA breaks were detected using TUNEL assay; scale bar represents 20 µm. **(C)** PARP activity was assayed in MOVAS cells. **(D)** NAD^+ concentrations were determined in MOVAS cells using an alcohol dehydrogenase-coupled colorimetric assay. ### indicate statistically significant difference between CTL and DOX/H_2O_2-treated samples, at $P<0.001$, * or *** indicate statistically significant difference between scPARP-2 cells and shPARP-2 cells at $P<0.05$ or <0.001, respectively. Error is represented as SD.

6.2.3. PARP-2 depletion and consequent SIRT1 overexpression counteracts DOX toxicity

The above described results suggest that the protection provided by the depletion of PARP-2 is based upon a different mechanism than the one responsible for the protective effect of PARP-1 inhibition during DOX treatment. It is well understood that mitochondrial function and structure is deteriorated upon DOX treatment (Yen et al., 1996). It has also been reported that the preservation of mitochondrial function is associated with protection

against DOX toxicity (Hasinoff et al., 2003; Tao et al., 2007; Xu et al., 2002). Therefore we intended to investigate pathways that modulate mitochondrial function.

SIRT1 activation promotes mitochondrial biogenesis (Baur et al., 2006; Lagouge et al., 2006; Rodgers et al., 2005). As we have described in the previous section, PARP-2 has been identified as a repressor of SIRT1 expression. It is tempting to assume therefore that the induction of SIRT1 provoked by PARP-2 depletion might be capable of counteracting DOX-evoked mitochondrial dsyfunction.

Disruption or depletion of PARP-2 in aortae (**Figure 14A.**) or in MOVAS cells (**Figure 14B.**) resulted in an increase in SIRT1 mRNA and SIRT1 protein levels (**Figures 14C and 14D.**). That was due to the induction of the SIRT1 promoter (**Figure 14F.**) induced by decreased promoter occupancy by PARP-2 (**Figure 14E.**).

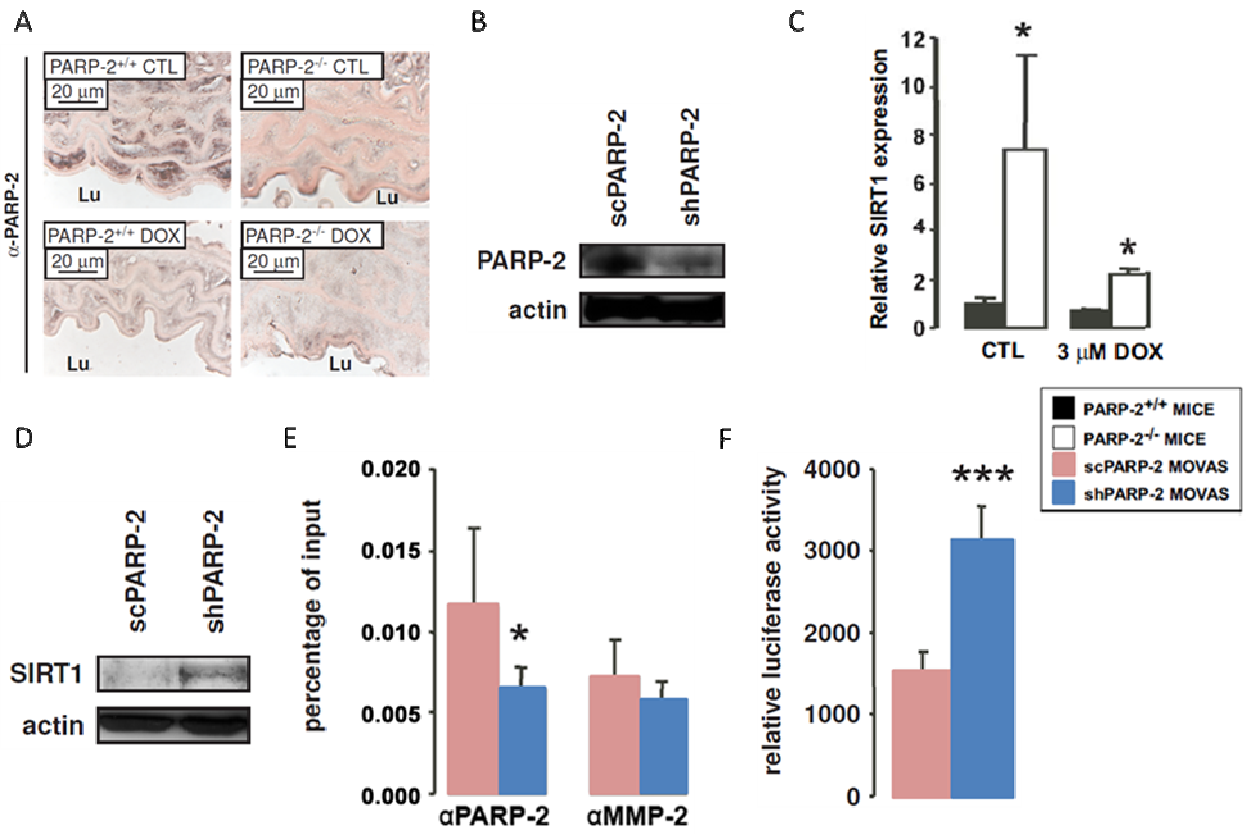

Figure 14. Depletion of PARP-2 induces SIRT1 expression in aortic smooth muscle cells. *PARP-2*$^{+/+}$ and *PARP-2*$^{-/-}$ mice were injected with saline (CTL) or with DOX at 3 months of age (n=7, 5, 5, and 5, respectively), and then aortic samples were collected on day 2 (A and C). An aortic smooth muscle cell line (MOVAS) was also tested (B, D, E and F). MOVAS cells were transduced with a PARP-2-silencing (shPARP-2) or –scrambled (scPARP-2) shRNA and treated with solvent (CTL) or DOX. **(A)** PARP-2 expression was determined in aortae by immunohistochemistry, scale bar represents 20 µm, and **(B)** in MOVAS cells by western blotting. **(C)** SIRT1 expression was determined in aortas by RT-qPCR, while **(D)** in MOVAS cells by western blotting. **(E)** PARP-2 binding to the SIRT1 promoter was determined using ChIP assays (n=3). **(F)** The activity of the ¯1 to ¯91 portion of the SIRT1 promoter was determined in luciferase assays (n=6). Lu, lumen, * and *** indicate statistically significant difference between scPARP-2 cells/*PARP-2*$^{+/+}$ mice vs. shPARP-2 cells/*PARP-2*$^{-/-}$ mice at P<0.05 or <0.001, respectively. On (E) and (F), error is represented as SD.

Consequently, mitochondrial DNA content increased both in aortae (**Figure 15A.**) and in MOVAS cells (**Figure 15C.**) upon a decrease in PARP-2 expression. Increased expression of genes involved in biological oxidation also pointed towards increased mitochondrial biogenesis (**Figure 15B.**). The boost in oxidative gene expression was maintained in *PARP-2*$^{-/-}$ mice even after DOX treatment compared with the wild type animals. To further support our hypothesis on increased mitochondrial activity we set out investigating mitochondrial membrane potential and oxygen consumption in MOVAS cells upon DOX treatment. DOX treatment induced a gradual decrease in cellular oxygen consumption (**Figure 15D.**),

indicative of DOX-induced mitochondrial dysfunction. In the absence of DOX shPARP-2 cells had a tendency towards higher oxygen consumption rate, as compared to scPARP-2 cells. DOX treatment for 7 hours accentuated the difference between sc and shPARP-2 cells (**Figure 15D.**). Moreover, since PARP-2 depletion enhanced mitochondrial biogenesis, it proved to be protective against DOX-induced mitochondrial damage. In line with these observations, DOX treatment enhanced free radical production (**Figure 13A.**) also indicative of mitochondrial uncoupling and damage. Mitochondrial membrane potential in scPARP-2 MOVAS cells increased in line with DOX concentration (**Figure 15E.**), pointing to mitochondrial hyperpolarization, that has been described as an early event in apoptosis (Scarlett et al., 2000) further supporting impaired mitochondrial biogenesis. The shPARP-2 cells were protected against mitochondrial hyperpolarization that equally points towards retained mitochondrial function upon DOX treatment (**Figure 15E.**).

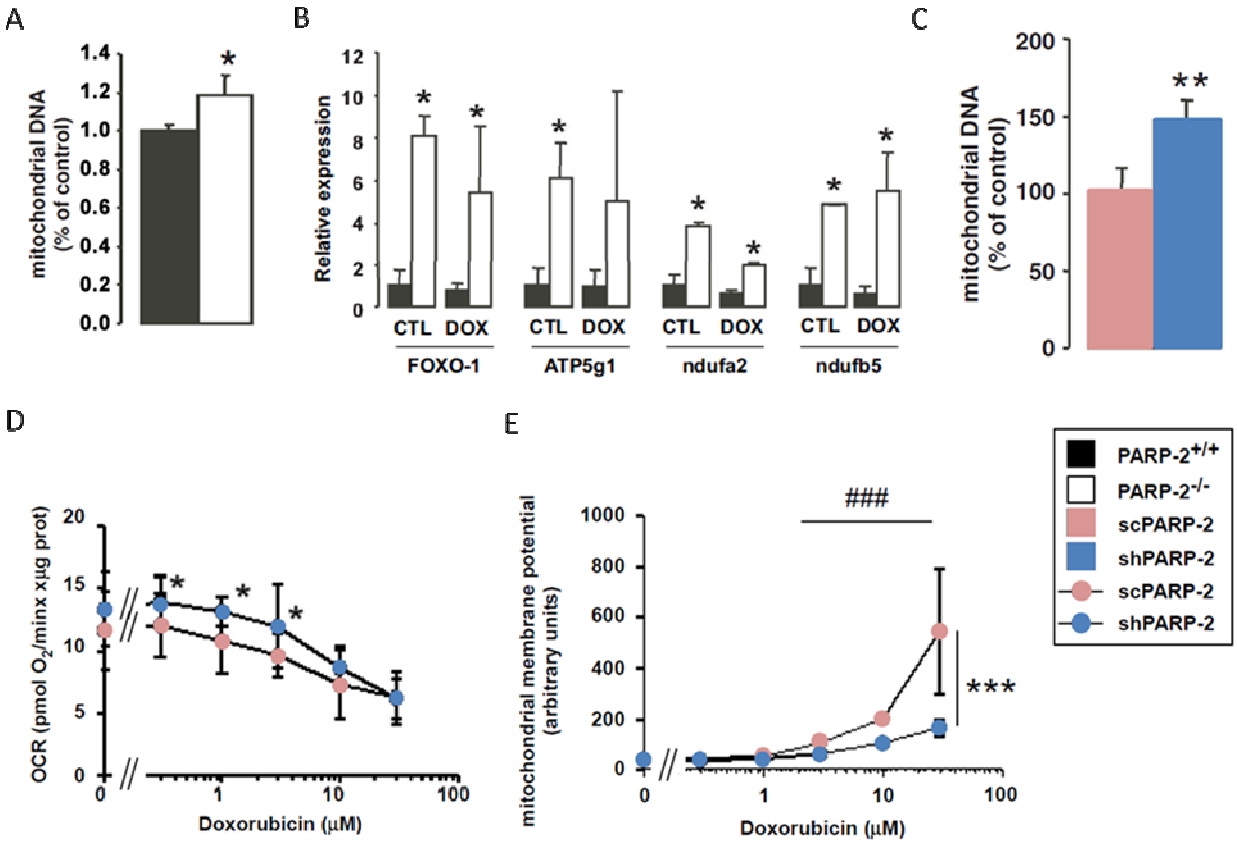

Figure 15. PARP-2 regulates mitochondrial function: possible involvement of SIRT1. *PARP-2*$^{+/+}$ and *PARP-2*$^{-/-}$ mice (3 months of age) were injected with saline (CTL) or with DOX (n=7 for *PARP-2*$^{+/+}$ CTL, n=5 for *PARP-2*$^{-/-}$ CTL, n=5 for *PARP-2*$^{+/+}$ DOX, and n=7 for *PARP-2*$^{-/-}$ DOX), and then aortic samples were collected on day 2 (A and B). An aortic smooth muscle cell line (MOVAS) was also tested (C, D and E). MOVAS cells (n=3 parallel measurements) transduced with a PARP-2-silencing (shPARP-2) or -scrambled (scPARP-2) shRNA were treated with solvent (CTL) or DOX (3 µM). **(A and C)** Mitochondrial DNA content was determined by qPCR. **(B)** Expression of a set of mitochondrial genes was determined by RT-qPCR. **(D)** Oxygen consumption rate of MOVAS cells was measured. **(E)** Membrane potential was determined using TMRE dye. ### indicate statistically significant difference between DOX-treated samples and their respective controls, at P<0.001; *, ** and *** indicate statistically significant difference between *PARP-2*$^{+/+}$ mice/scPARP-2 cells vs. *PARP-2*$^{-/-}$ mice/shPARP-2 cells at P<0.05, <0.01 and <0.001, respectively. On (C) and (D), error is presented as SD.

7. DISCUSSION

7.1. PARP-2 regulates SIRT1 expression

Our work was initiated by some intriguing metabolic features of the *PARP-2*$^{-/-}$ mice. *PARP-2*$^{-/-}$ mice were smaller and leaner than their *PARP-2*$^{+/+}$ littermates (Bai et al., 2011[a]). At the same time, *PARP-2*$^{-/-}$ mice showed higher oxygen consumption rates pointing towards higher oxidation rates as compared to the wild type mice (Bai et al., 2011[a]). Increased whole-body energy expenditure (EE) stemmed from higher mitochondrial content of skeletal muscle fibers and had effects on the metabolism of the *PARP-2*$^{-/-}$ mice. *PARP-2*$^{-/-}$ mice were protected against diet-induced obesity and insulin sensitivity of the knock-out animals was retained even after high fat feeding (Bai et al., 2011[a]). Multiple studies reported that the activation of SIRT1 in mice results in higher EE and protection against high fat diet (HFD)-induced obesity (Cantó et al., 2009; Lagouge et al., 2006). Taken together, *PARP-2*$^{-/-}$ mice phenocopied the effects of SIRT1 activation.

Studies demonstrated a link between PARP-1, the major PARP activity in most tissues, and SIRT1 activity (Kolthur-Seetharam et al., 2006; Pillai et al., 2005). Since PARP-1 activity critically influences NAD^+ bioavailability (Sims et al., 1981), and SIRT1 activity is dependent on cellular NAD^+ content, PARP-1 and SIRT1 are linked through competing for the limiting NAD^+ pool (Bai et al., 2011[b]). The fact that PARP-2 has a catalytic domain structurally very similar to that of PARP-1, and the potential relevance of PARP-2 for NAD^+ homeostasis furthered the assumption that PARP-2 depletion might act on SIRT1 activity.

In our studies we have shown that the lack of PARP-2 activates SIRT1 and promotes mitochondrial metabolism. However, unlike PARP-1, the impact of PARP-2 on SIRT1 activity is not necessarily based on changes in NAD^+ content. This is in line with the previous observations that PARP-2 represents only a minor PARP activity in cells (Amé et al., 1999; Shieh et al., 1998), therefore probably it does not have significant influence on NAD^+ homeostasis. Our data identify PARP-2 as a repressor of the SIRT1 promoter. This was strengthened by increased SIRT1 mRNA expression, protein content and activity upon PARP-2 depletion or deletion in various models and tissues tested [Fig. 1D, 3C, 3D, 3E, 4E, 6H in (Bai et al., 2011[a])].

Indeed, PARP-2 can act as a transcriptional regulator. In the thymus of *PARP-2*$^{-/-}$ mice, an increased expression of the proapoptotic protein NOXA was observed (Yélamos et al.,

2006). In cultured lung epithelial cells PARP-2 has been shown to interact with TTF-1 and hence PARP-2 regulates the expression of surfactant protein-B (Maeda et al., 2006). Moreover, our group has previously reported that PARP-2 is a positive regulator of PPARγ, therefore its absence impairs fat accumulation (Bai et al., 2007). SIRT1 induction may provide an auxiliary mechanism to decrease lipid accumulation *in vivo*. SIRT1 overexpression reportedly reduces fat accumulation and the expression of genes encoding important fat-storage proteins, such as aP2, PPARγ, and CCAAT/enhancer-binding protein α and δ (C/EBP α and δ) (Picard et al., 2004). In line with this, our group has shown that PARP-2 deficiency led to decreased lipid accumulation [Fig. 5C, 5D in (Bai et al., 2011[a])].

In summary, we provided data that expand the role of PARP-2 as a repressor of the SIRT1 promoter. Accordingly, deletion of PARP-2 has the ability to induce SIRT1 transcription and mitochondrial metabolism (**Figure 16.**).

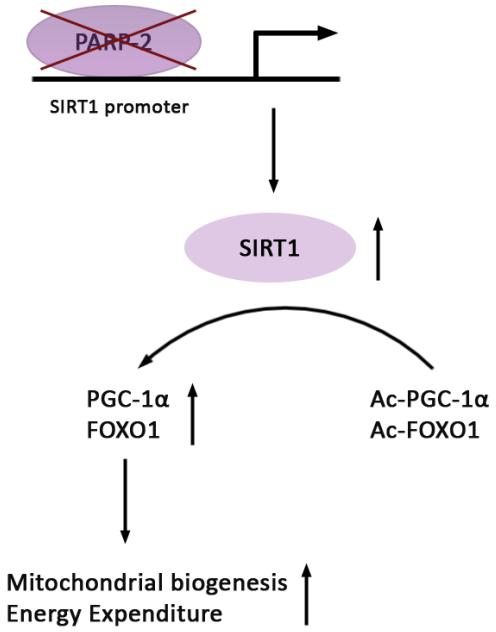

Figure 16. PARP-2 influences SIRT1 activity. The scheme illustrates how the depletion of PARP-2 can activate SIRT1 function. PARP-2 acts as a negative regulator of the SIRT1 promoter. The absence of PARP-2 promotes SIRT1 activity and enhances mitochondrial metabolism.

The actual molecular mechanism(s) through which PARP-2 impacts on gene transcription is yet to be uncovered. It has been reported that PARP-1 binding to nucleosomes in the absence of NAD^+ promotes the compaction of nucleosomal arrays into

higher order structure (Kraus, 2008). In the presence of saturating amounts of NAD^+, PARP-1 automodifies and releases from chromatin, leading to decompaction and the restoration of transcription (Kraus, 2008). Assuming similar role of PARP-2 in genome remodeling and in the modulation of chromatin structure as PARP-1, it might be possible that PARP-2 acts in a similar way in the regulation of SIRT1 transcription. Since the enzymatic activity of PARPs requires a ready supply of NAD^+, intense SIRT1 activity could hamper the maintenance of PARP functions, for example under conditions of severe DNA damage. It might be possible that PARP-2 repress SIRT1 transcription when NAD^+ content becomes very limited to serve the needs of both PARPs and SIRT1. PARylation of histones by PARP-2 is also a plausible mode of action in the PARP-2-mediated regulation of transcription. Furthermore, PARP-2 activity may remove components of the regulatory complex by PARylation of the individual proteins. PARylation and consequent inactivation of certain transcription factors involved in SIRT1 transcription (e.g. p53) (Nemoto et al., 2004) might also be possible. Besides, our model proposes a possible feedback regulation of PARP-2 by SIRT1, since acetylation is a possible posttranslational modification of PARP-2 reducing its DNA-binding and enzymatic activity (Haenni et al., 2008). Therefore SIRT1 might deacetylate PARP-2 and thereby increase its DNA-binding which would limit SIRT1 transcription.

It is of note though, that the interaction of PARP-2 and the promoter region of *SIRT1* gene has been detected in cultured myotubes, skeletal muscle, liver and smooth muscle, therefore it seems to be a widespread mechanism and probably of phylogenetic significance. Especially as that PARP-2 binds to the very proximal region of the SIRT1 promoter (region between the transcription start site and -91 bp), which is extremely conserved along the evolution, showing homology even in Xenopus (**Figure 17.**). However, the fact that in certain organs depletion of PARP-2 does not induce EE (e.g. brown adipose tissue) suggests that auxiliary mechanisms might be needed to couple SIRT1 induction to EE.

Figure 17. Alignment of the SIRT1 promoter of different vertebrate species was performed using the ClustalW software. The green field indicates the murine ⁻1 - ⁻91 region, where PARP-2 binds. *Adapted from: Bai et al., 2011[a].*

Nevertheless, PARP-2 depletion unites all the beneficial effects previously observed upon triggering SIRT1 activation by various means, such as enhanced oxidative metabolism, endurance phenotype, protection against body weight gain (Bai et al., 2011[a], Feige et al., 2008; Lagouge et al., 2006). Therefore hereby we suggest the possible utilization of PARP-2 inhibitors to activate SIRT1 and promote oxidative metabolism which could be exploited in the management of metabolic diseases.

7.2. PARP-2 depletion reduces DOX-induced damage through SIRT1 induction

DOX therapy causes cardiovascular dysfunction as a side effect (Singal and Iliskovic, 1998). DOX treatment has been shown to affect endothelial functions in the vasculature (Murata et al., 2001) and there are data about the deleterious effects of DOX affecting cardiac tissues (Bai et al., 2004). However, the vascular effects of DOX, especially smooth muscle-specific ones, are largely unknown.

We investigated vascular functions after DOX treatment in *PARP-2*$^{+/+}$ and in *PARP-2*$^{-/-}$ mice. Aorta ring studies showed that upon DOX treatment endothelial and smooth muscle functions are damaged. The deterioration of endothelial function in DOX-treated animals

seems to be PARP-independent, at least 2-days post-treatment [(Fig. 1A, 1B, 1C, 1D and 1E in (Szántó et al., 2011)]. However, the deletion of PARP-2 protected the aortic smooth muscle against the dysfunction induced by DOX. We aimed to explore the possible mechanism by which the absence of PARP-2 provided protection against DOX-evoked smooth muscle damage. Since DOX triggers PARP activation, the inhibition of which is protective against DOX toxicity (Pacher et al., 2002; Pacher et al., 2006), we hypothesized whether the deletion of PARP-2 hampered DOX-induced PARP-activation and thereby provided protection. However, our results clearly show that the deletion or depletion of PARP-2 did not alter DOX-induced free radical formation and the consequent DNA breakage that leads to PARP-1 activation and NAD^+ depletion in smooth muscle cells. In other words, the deletion or depletion of PARP-2 protected the vascular smooth muscle cells against DOX-induced damage without interfering in the PARP activation and the consequent NAD^+ depletion.

In seeking a possible alternative mechanism by which PARP-2 depletion attenuated DOX-induced damage, we have examined mitochondrial functions. Since cardiovascular injury associated with DOX treatment is characterized by the disruption of mitochondrial membranes (Davies and Doroshow, 1986), the preservation of mitochondrial functions is protective against DOX toxicity (Yen et al., 1996; Hasinoff et al., 2003; Tao et al., 2007; Xu et al., 2002; Danz et al., 2009). We have demonstrated that PARP-2 depletion is associated with the induction of mitochondrial activity through the induction of SIRT1 transcription, probably followed by increased SIRT1 activity. Increased SIRT1 activity results in advantageous effects (e.g. enhanced mitochondrial respiration, oxidative capacity and mitochondrial biogenesis) that are able to stabilize mitochondrial functions. Indeed, the aortae of *PARP-2*$^{-/-}$ mice and PARP-2 knock-down aortic smooth muscle cells displayed increased SIRT1 expression and SIRT1 protein content which was the consequence of the decreased occupancy of the SIRT1 promoter by PARP-2. In consequence of higher SIRT1 level, probably augmented deacetylating capacity of SIRT1 boosted the mitochondrial metabolism, which probably contributed to the protective phenotype against vascular DOX toxicity that evolved upon the lack of PARP-2. Enhanced mitochondrial biogenesis, induced by PARP-2 depletion, may be able to counterbalance the DOX-induced loss of mitochondrial activity and provides a new approach to counteract the oxidative stress-evoked damage in blood vessels (**Figure 18.**).

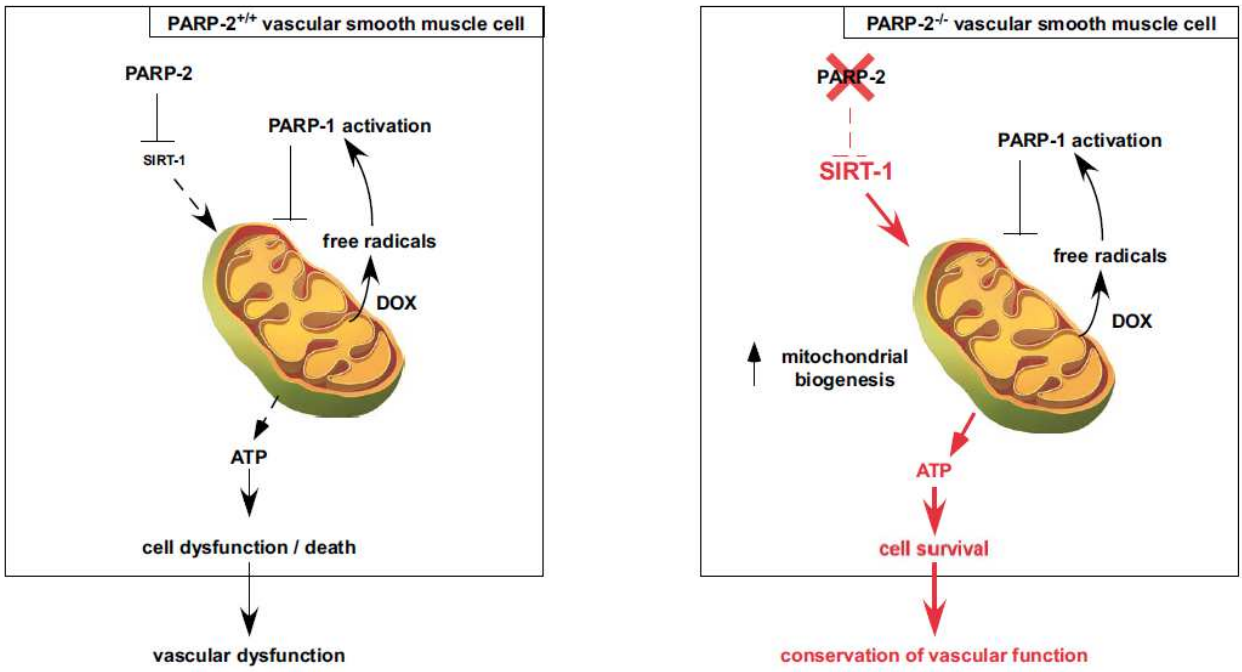

Figure 18. Proposed mechanism for PARP-2-dependent protection against DOX-evoked vascular dysfunction. PARP-2 down-regulation evokes an increase in SIRT1 expression, which results in the activation of mitochondrial biogenesis. Elevated mitochondrial function protects aortic smooth muscle from DOX-induced toxicity without affecting PARP-1-mediated functions.

Indeed, SIRT1 induction has been shown to act as a cardioprotective factor (Danz et al., 2009; Alcendor et al., 2007; Borradaile et al., 2009; Pillai et al., 2005; Rajamohan et al., 2009), but this is the first time when the protective properties of SIRT1-induced mitochondrial biogenesis have been identified in blood vessels. Moreover, this is the first time when SIRT1 induction was achieved by direct transcriptional regulation by the depletion of PARP-2. It is of note though, that SIRT1 induction can activate other protective mechanisms in the heart. It may deacetylate p53 and induce the expression of Bax family proteins (Zhang et al., 2011). SIRT1 may also impair PARP-1 activation and the consequent cellular dysfunction through deacetylating PARP-1 (Rajamohan et al., 2009), or by consuming NAD^+ (Pillai et al., 2005). However, we did not observe differences in PARP activity or NAD^+ consumption in PARP-2-depleted smooth muscle cells or in *PARP-2*$^{-/-}$ aortae, but we did observe an up-regulation of SIRT1 and increased mitochondrial function. These apparent differences suggest that the mechanism of vascular protection may consist of different pathways than those observed in the heart. Nevertheless, the preservation of mitochondrial functions seems to be an essential element in protection against DOX-induced dysfunction.

It is tempting to speculate that SIRT1-mediated induction of mitochondrial biogenesis may also have contributed to the protective phenotype upon PARP-2 depletion in oxidative stress-mediated diseases such as colitis (Popoff et al., 2002) or cerebral ischemia (Kofler et al., 2006; Moroni et al., 2009) and could be exploited in other oxidative stress-related diseases.

Our data prompt the speculation that PARP-2 specific inhibitors could be applied as vascular protective agents and therefore point towards the importance of their development. In current therapeutic protocols, dexrazoxane hydrochloride (Cardioxane, Novartis) is used to circumvent DOX-induced cardiovascular damage. However, in July 2011 the US Food and Drug Administration released a statement restricting its use only in adult patients with breast cancer who have received >300 mg/m^2 doxorubicin and general approval for use for cardiovascular protection was withdrawn since clinical trials showed higher rates of secondary malignancies and acute myelogenous leukemia in pediatric patients treated with dexrazoxane. The use of PARP-2 specific inhibitors might therefore offer an alternative solution for the effective protection of the vasculature in DOX-treated patients.

All known PARP inhibitors are understood to be able to inhibit both PARP-1 and -2. This is not surprising since the catalytic domains of PARP-1 and PARP-2 are very similar (**Figure 4.**) and most PARP inhibitors bind there (Oliver et al., 2004; Karlberg et al., 2010). Seeking highly PARP-2 selective compounds have given rise to inhibitors that have 10-60 fold preference towards PARP-2 compared to PARP-1 (Ishida et al., 2006; Iwashita et al., 2005; Pellicciari et al., 2008; Sunderland et al., 2011; Moroni et al., 2009). UPF-1069, that inhibits PARP-2 with 60 fold higher affinity than it does PARP-1, was effective in protecting cultured mouse cortical neurons against cerebral ischemia (Moroni et al., 2009). Unfortunately, at the moment such selectivity is the highest achievable. It is possible that in cells or in *in vivo* settings these inhibitors may partially inhibit PARP-1, too. Therefore the development of highly PARP-2 specific inhibitors is of current interest and of great significance. Since PARP-2 is a minor PARP isoform and accounts for only 5-15% of total PARP activity (Amé et al., 1999; Schreiber et al., 2002; Shieh et al., 1998), its loss probably does not hamper PARP-driven DNA repair drastically. Thus using highly PARP-2 specific inhibitors may counteract certain drawbacks of pan-PARP inhibition or PARP-1 specific inhibitors.

In summary, we propose that modulation of the PARP-2 - SIRT1 axis to enhance mitochondrial activity may be a new therapeutic approach to revert mitochondrial hypofunction in the cardiovascular system or in other organs.

8. SUMMARY

PARP-2 is a PARP enzyme that participates in multiple cellular processes and is activated upon DNA strand breaks. PARP-1, that covers most PARP activity in cells, is a DNA-damage dependent enzyme and a major cellular NAD^+ consumer. In the nucleus PARP-1 competes with SIRT1, an NAD^+-dependent deacetylase, for the limited NAD^+ pool. Therefore, the deletion or inhibition of PARP-1 promotes SIRT1 activation. Increased SIRT1 activity, results in increased mitochondrial biogenesis and fatty acid oxidation, higher energy expenditure in several organs, resulting in protection against high fat diet-induced obesity. Since PARP-2 is a PARP enzyme and consumes nuclear NAD^+, we aimed to explore a possible link between PARP-2 and SIRT1, and thereby between PARP-2 and the mitochondrial metabolism. Here we have shown that this link does exist, however unlike in the case of PARP-1, this interaction is not based on changes in NAD^+ levels. Rather, PARP-2 acts as a transcriptional repressor of SIRT1. Therefore, the depletion of PARP-2 leads to enhanced SIRT1 activity and thereby increased mitochondrial metabolism. Increased SIRT1 activity is also able to stabilize mitochondrial functions.

Oxidative stress-related pathologies, such as doxorubicin (DOX)-induced vascular damage, are associated with mitochondrial damage. Restoring mitochondrial activity is proved to be successful in counteracting mitochondrial injury caused by increased oxidative stress and free radical production. PARP-2 depletion has been associated with protection against oxidative stress-related pathologies (e.g. colitis or cerebral ischemia)-induced damage. Hereby we have shown that the deletion or depletion of PARP-2 provided protection against DOX-induced deterioration of vascular smooth muscle function. It has been accomplished by the preservation of mitochondrial functions due to enhanced SIRT1 transcription induced by decreased SIRT1 promoter occupancy by PARP-2.

We suggest the exploitation of the PARP-2 - SIRT1 interaction in the management of metabolic diseases, and also in counteracting the oxidative stress-related tissue injury and cell dysfunction. Our data therefore spotlight the importance of developing PARP-2 specific inhibitors.

9. ÖSSZEFOGLALÁS

A PARP-2 a PARP enzimek családjába tartozó enzim, mely számos sejten belüli folyamatban játszik szerepet, és DNS törések indukálják. Szintén a DNS törés az elsődleges aktivátora a PARP-1-nek, mely a legaktívabb PARP enzim, így a sejtek NAD^+ készletének jelentős felhasználója. A sejtmagban a PARP-1 aktivációja során ugyanazt a NAD^+ készletet használja, mint a SIRT1 enzim, amely deacetiláz tulajdonsággal bír. Ennél fogva a PARP-1 genetikai delécióját vagy gátlása a SIRT1 aktivitásának növekedésével jár. Intenzív SIRT1 aktiváció hatására növekszik a sejtekben a mitokondriális biogenesis és zsírsav oxidáció, ami összességében nagyobb energia felhasználást eredményez, és védelmet nyújt a magas zsírtartalmú táplálkozás következtében kialakuló elhízással szemben. Mivel a PARP-2 PARP enzim lévén NAD^+-ot használ, célul tűztük ki, hogy megvizsgáljuk, van-e valamilyen kapcsolat a PARP-2 és a SIRT1, és ezáltal a PARP-2 és a mitokondriális metabolizmus között. Jelen tanulmány keretei között megmutattuk, hogy ez a kapcsolat létezik. Azonban a PARP-1-gyel ellentétben a PARP-2 nem a sejtmag NAD^+-készletén keresztül szabályozza a SIRT1 aktivitását, hanem transzkripciós szinten. A PARP-2 a SIRT1 promoterének represszoraként működik. Ezáltal a PARP-2 depléciója a SIRT1 aktivitásának, valamint a mitokondriális metabolizmus fokozódását eredményezi. A SIRT1 aktivitásának növekedése hozzájárulhat a mitokondriális funkciók stabilizálásához is.

A sejtekben oxidatív stresszt kiváltó kórképek, köztük a doxorubicin (DOX) által okozott vaszkuláris károsodás, mitokondriális károsodást okoznak. A mitokondriális funkciók helyreállítása hatékony stratégia ennek a hatásnak a kivédésében. A PARP-2 depléciója védelmet nyújt a kolitisz, illetve a cerebrális iszkémia reperfúzió következtében kialakuló oxidatív stressz károsító hatásaival szemben. Kutatásaink során bebizonyítottuk, hogy a PARP-2 delécióját vagy depléciója védelmet biztosít a DOX által okozott vaszkuláris simaizom károsodással szemben is. Ezen hatás hátterében az áll, hogy a SIRT1 promotere felszabadult a PARP-2 általi gátlás alól, így a SIRT1 transzkripciójának fokozódása nyomán a mitokondriális funkciók stabilizálódtak.

Eredményeink alapján javasoljuk a PARP-2 inhibitorok alkalmazását metabolikus kórképek terápiájában, valamint az oxidatív stressz által okozott káros hatások csökkentésére, egyúttal felhívjuk a figyelmet a PARP-2 specifikus inhibitorok fejlesztésének fontosságára.

10. REFERENCES

Alcendor RR, Gao S, Zhai P, Zablocki D, Holle E, Yu X, Tian B, Wagner T, Vatner SF, Sadoshima J (2007). Sirt1 regulates aging and resistance to oxidative stress in the heart. *Circulation Research* 100(10):1512-1521.

Altmeyer M, Messner S, Hassa PO, Fey M, Hottiger MO (2009) Molecular mechanism of poly(ADP-ribosyl)ation by PARP1 and identification of lysine residues as ADP-ribose acceptor sites. *Nucleic Acids Research* 37(11):3723-3738.

Amé JC, Rolli V, Schreiber V, Niedergang C, Apiou F, Decker P, Muller S, Hoger T, Menissier-de Murcia J, and de Murcia G (1999). PARP-2, a novel mammalian DNA damage-dependent poly(ADP-ribose) polymerase. *The Journal of Biological Chemistry* 274:17860–17868.

Amé JC, Schreiber V, Fraulob V, Dolle P, de Murcia G, Niedergang CP (2001). A bidirectional promoter connects the poly(ADP-ribose) polymerase 2 (PARP-2) gene to the gene for RNase P RNA. structure and expression of the mouse PARP-2 gene. *The Journal of Biological Chemistry* 276(14):11092-11099.

Amé JC, Spenlehauer C, de Murcia G (2004). The PARP superfamily. *Bioessays* 26:882-893.

Bai P, Bakondi E, Szabó É, Gergely P, Szabó C, Virág L (2001). Partial protection by poly(ADP-ribose) polymerase inhibitors from nitroxyl-induced cytotoxicity in thymocytes. *Free Radical Biology and Medicine* 31(12): 1616-1623.

Bai P, Mabley JG, Liaudet L, Virág L, Szabó C, Pacher P (2004). Matrix metalloproteinase activation is an early event in doxorubicin-induced cardiotoxicity. *Oncology Reports* 11(2):505-508.

Bai P, Houten SM, Huber A, Schreiber V, Watanabe M, Kiss B, de Murcia G, Auwerx J, Ménissier-de Murcia J (2007). Poly(ADP-ribose) polymerase-2 (PARP)-2 controls adipocyte differentiation and adipose tissue function through the regulation of the activity of the

retinoid X receptor/PPARγ heterodimer. *The Journal of Biological Chemistry* 282(52):37738–37746.

Bai P, Canto C, Brunyánszki A, Huber A, Szántó M, Cen Y, Yamamoto H, Houten SM, Kiss B, Oudart H, Gergely P, Menissier-de Murcia J, Schreiber V, Sauve AA, Auwerx J (2011)[a]. PARP-2 regulates SIRT1 expression and whole-body energy expenditure. *Cell Metabolism* 13(4):450-460.

Bai P, Cantó C, Oudart H, Brunyánszki A, Cen Y, Thomas C, Yamamoto H, Huber A, Kiss B, Houtkooper RH, Schoonjans K, Schreiber V, Sauve AA, Ménissier-de Murcia J, Auwerx J (2011)[b]. PARP-1 inhibition increases mitochondrial metabolism through SIRT1 activation. *Cell Metabolism* 13:461-468.

Bardot O, Aldridge TC, Latruffe N, Green S (1993). PPAR-RXR heterodimer activates a peroxisome proliferator response element upstream of the bifunctional enzyme gene. *Biochemical and Biophysical Research Commununications* 192(1):37-45.

Baur JA, Pearson KJ, Price NL, Jamieson HA, Lerin C, Kalra A Prabhu VV, Allard JS, Lopez-Lluch G, Lewis K, Pistell PJ, Poosala S, Becker KG, Boss O, Gwinn D, Wang M, Ramaswamy S, Fishbein KW, Spencer RG, Lakatta EG, Le Couteur D, Shaw RJ, Navas P, Puigserver P, Ingram DK, de Cabo R, Sinclair DA (2006). Resveratrol improves health and survival of mice on a high-calorie diet. *Nature* 444:337–342.

Benchoua A, Couriaud C, Guégan C, Tartier L, Couvert P, Friocourt G, Chelly J, Ménissier-de Murcia J, Onténiente B (2002). Active caspase-8 translocates into the nucleus of apoptotic cells to inactivate poly(ADP-ribose) polymerase-2. *The Journal of Biological Chemistry* 277(37):34217-34222.

Berger NA (1985). Poly(ADP-ribose) in the cellular response to DNA damage. *Radiation research* 101:4-15.

Blander G, Guarente L (2004). The Sir2 family of protein deacetylases. *Annual Review of Biochemistry* 73:417-435.

Boehler C, Gauthier LR, Mortusewicz O, Biard DS, Saliou JM, Bresson A, Sanglier-Cianferani S, Smith S, Schreiber V, Boussin F, Dantzer F (2011). Poly(ADP-ribose) polymerase 3 (PARP3), a newcomer in cellular response to DNA damage and mitotic progression. *Proceedings of the National Academy of Sciences of the United States of America* 108:2783-2788.

Bohinski RJ, Di Lauro R, Whitsett JA (1994). The lung-specific surfactant protein B gene promoter is a target for thyroid transcription factor 1 and hepatocyte nuclear factor 3, indicating common factors for organ-specific gene expression along the foregut axis. *Molecular and Cellular Biology* 14(9):5671-5681.

Borradaile NM, Pickering JG (2009). NAD(+), sirtuins, and cardiovascular disease. *Current Pharmaceutical Design* 15(1):110-117.

Brunet A, Sweeney LB, Sturgill JF, Chua KF, Greer PL, Lin Y, Tran H, Ross SE, Mostoslavsky R, Cohen HY, Hu LS, Cheng HL, Jedrychowski MP, Gygi SP, Sinclair DA, Alt FW, Greenberg ME (2004). Stress-dependent regulation of FOXO transcription factors by the SIRT1 deacetylase. *Science* 303(5666):2011-2015.

Cantó C, Gerhart-Hines Z, Feige JN, Lagouge M, Noriega L, Milne JC, Elliott PJ, Puigserver P, Auwerx J (2009). AMPK regulates energy expenditure by modulating NAD+ metabolism and SIRT1 activity. *Nature* 458(7241):1056-1060.

Cantó C, Auwerx J (2012). Targeting sirtuin 1 to improve metabolism: all you need is NAD(+)? *Pharmacological Reviews* 64(1):166-187.

D'Amours D, Desnoyers S, D'Silva I, Poirier G (1999). Poly(ADPribosyl)ation reactions in the regulation of nuclear functions. *Biochemical Journal* 342:249-268.

Dantzer F, Giraud-Panis MJ, Jaco I, Amé JC, Schultz I, Blasco M, Koering CE, Gilson E, Ménissier-de Murcia J, de Murcia G, Schreiber V. (2004) Functional interaction between poly(ADP-Ribose) polymerase 2 (PARP-2) and TRF2: PARP activity negatively regulates TRF2. *Molecular and Cellular Biology* 24(4):1595-1607.

Dantzer F, Mark M, Quenet D, Scherthan H, Huber A, Liebe B, Monaco L, Chicheportiche A, Sassone-Corsi P, de Murcia G, Ménissier-de Murcia J (2006). Poly(ADP-ribose) polymerase-2 contributes to the fidelity of male meiosis I and spermiogenesis. *PNAS* 103(40):14854–14859.

Danz ED, Skramsted J, Henry N, Bennett JA, Keller RS (2009). Resveratrol prevents doxorubicin cardiotoxicity through mitochondrial stabilization and the Sirt1 pathway. *Free Radical Biology and Medicine* 46:1589–1597.

Davies KJ, Doroshow JH (1986). Redox cycling of anthracyclines by cardiac mitochondria. I. Anthracycline radical formation by NADH dehydrogenase. *The Journal of Biological Chemistry* 261:3060-3067.

Derenzini M (2000). The AgNORs. *Micron* 31(2):117-120.

Doroshow JH, Davies KJ (1986). Redox cycling of anthracyclines by cardiac mitochondria. II. Formation of superoxide anion, hydrogen peroxide, and hydroxyl radical. *The Journal of Biological Chemistry* 261:3068-3074.

Doucet-Chabeaud G, Godon C, Brutesco C, de Murcia G, Kazmaier M. Ionising radiation induces the expression of PARP-1 and PARP-2 genes in Arabidopsis (2001). *Molecular Genetics and Genomics* 265(6):954-963.

Dreyer C, Keller H, Mahfoudi A, Laudet V, Krey G, Wahli W (1993). Positive regulation of the peroxisomal beta-oxidation pathway by fatty acids through activation of peroxisome proliferator-activated receptors (PPAR). *Biology of the Cell* 77(1):67-76.

Evans RM, Barish GD, Wang YX (2004). PPARs and the complex journey to obesity. *Nature Medicine* 10(4):355-361.

Fajas L, Auboeuf D, Raspé E, Schoonjans K, Lefebvre AM, Saladin R, Najib J, Laville M, Fruchart JC, Deeb S, Vidal-Puig A, Flier J, Briggs MR, Staels B, Vidal H, Auwerx J (1997). The organization, promoter analysis, and expression of the human PPARgamma gene. *The Journal of Biological Chemistry* 272(30):18779-18789.

Feige JN, Lagouge M, Canto C, Strehle A, Houten SM, Milne JC, Lambert PD, Mataki C, Elliott PJ, Auwerx J (2008). Specific SIRT1 activation mimics low energy levels and protects against diet-induced metabolic disorders by enhancing fat oxidation. *Cell Metabolism* 8(5):347-358.

Fisher AE, Hochegger H, Takeda S, Caldecott KW (2007). Poly(ADP-ribose) polymerase 1 accelerates single-strand break repair in concert with poly(ADP-ribose) glycohydrolase. *Molecular and Cellular Biology* 27(15):5597-5605.

Forman BM, Chen J, Evans RM (1996). The peroxisome proliferator-activated receptors: ligands and activators. *Annals of The New York Academy of Sciences* 804:266-275.

Fuentes-Mascorro G, Serrano H, Rosado A (2000). Sperm chromatin. *Archives of Andrology* 45(3):215-225.

Géhl Zs, Bai P, Bodnár E, Emri G, Remenyik É, Németh J, Gergely P, Virág L, Szabó É (2012). Poly(ADP-ribose) in the skin and in melanomas. Histology and Histopathology 27(5):651-659.

Haenni SS, Altmeyer M, Hassa PO, Valovka T, Fey M, Hottiger MO (2008). Importin alpha binding and nuclear localization of PARP-2 is dependent on lysine 36, which is located within a predicted classical NLS. *BMC Cell Biology* 9:39.

Haenni SS, Hassa PO, Altmeyer M, Fey M, Imhof R, Hottiger MO (2008). Identification of lysines 36 and 37 of PARP-2 as targets for acetylation and auto-ADP-ribosylation. *International Journal of Biochemistry and Cell Biology* 40(10):2274-2283.

Hasinoff BB, Schnabl KL, Marusak RA, Patel D, Huebner E (2003) Dexrazoxane (ICRF-187) protects cardiac myocytes against doxorubicin by preventing damage to mitochondria. *Cardiovascular Toxicology* 3:89–99.

Hassa PO, Hottiger MO (2008). The diverse biological roles of mammalian PARPs, a small but powerful family of poly-ADP-ribose polymerases. *Frontiers in Bioscience* 13:3046-3082.

Houtkooper RH, Cantó C, Wanders RJ, Auwerx J (2010). The secret life of NAD^+: an old metabolite controlling new metabolic signaling pathways. *Endocrine Reviews* 31:194–223.

Howitz KT, Bitterman KJ, Cohen HY, Lamming DW, Lavu S, Wood JG, Zipkin RE, Chung P, Kisielewski A, Zhang LL, Scherer B, Sinclair DA (2003). Small molecule activators of sirtuins extend Saccharomyces cerevisiae lifespan. *Nature* 425(6954):191-196.

Huber A, Bai P, de Murcia JM, de Murcia G (2004). PARP-1, PARP-2 and ATM in the DNA damage response: functional synergy in mouse development. *DNA Repair* 3(8-9):1103-1108.

Imai S, Armstrong CM, Kaeberlein M, Guarente L (2000). Transcriptional silencing and longevity protein Sir2 is an NAD-dependent histone deacetylase. *Nature* 403(6771):795-800.

Isabelle M., Moreel X., Gagné JP., Rouleau M., Ethier C., Gagné P., Hendzel MJ., Poirier GG. (2010). Investigation of PARP-1, PARP-2, and PARG interactomes by affinity-purification mass spectrometry. *Proteome Science* 8:22.

Ishida J, Yamamoto H, Kido Y, Kamijo K, Murano K, Miyake H, Ohkubo M, Kinoshita T, Warizaya M, Iwashita A, Mihara K, Matsuoka N, Hattori K (2006). Discovery of potent and selective PARP-1 and PARP-2 inhibitors: SBDD analysis via a combination of X-ray structural study and homology modeling. *Bioorganic and Medicinal Chemistry* 14(5):1378-1390.

Iwashita A, Hattori K, Yamamoto H, Ishida J, Kido Y, Kamijo K, Murano K, Miyake H, Kinoshita T, Warizaya M, Ohkubo M, Matsuoka N, Mutoh S (2005). Discovery of quinazolinone and quinoxaline derivatives as potent and selective poly(ADP-ribose) polymerase-1/2 inhibitors. *FEBS Letters* 579(6):1389-1393.

Johansson M (1999). A human poly(ADP-ribose) polymerase gene family (ADPRTL): cDNA cloning of two novel poly(ADP-ribose) polymerase homologues. *Genomics* 57(3):442-445.

Ju BG, Lunyak VV, Perissi V, Garcia-Bassets I, Rose DW, Glass CK, Rosenfeld MG (2006). A topoisomerase IIb-mediated dsDNA break required for regulated transcription. *Science* 312(5781):1798-802.

Kang YH, Lee KA, Kim JH, Park SG, Yoon DY (2010). Mitomycin C modulates DNA-double strand break repair genes in cervical carcinoma cells. *Amino Acids* 39(5):1291-1298.

Karlberg T, Hammarström M, Schütz P, Svensson L, Schüler H (2010). Crystal structure of the catalytic domain of human PARP2 in complex with PARP inhibitor ABT-888. *Biochemistry* 49(6):1056-1058.

Kimura S, Hara Y, Pineau T, Fernandez-Salguero P, Fox CH, Ward JM, Gonzalez FJ (1996). The T/ebp null mouse: thyroid-specific enhancer-binding protein is essential for the organogenesis of the thyroid, lung, ventral forebrain, and pituitary. *Genes and Development* 10(1):60-69.

Kofler J, Otsuka T, Zhang Z, Noppens R, Grafe MR, Koh DW, Dawson VL, Ménissier-de Murcia J, Hurn PD, Traystman RJ (2006). Differential effect of PARP-2 deletion on brain injury after focal and global cerebral ischemia. *Journal of Cerebral Blood Flow and Metabolism* 26:135-141.

Kolthur-Seetharam U, Dantzer F, McBurney MW, de Murcia G, Sassone-Corsi P (2006). Control of AIF-mediated cell death by the functional interplay of SIRT1 and PARP-1 in response to DNA damage. *Cell Cycle* 5:873–877.

Kraus WL (2008). Transcriptional control by PARP-1: chromatin modulation, enhancer-binding, coregulation, and insulation. *Current Opinions in Cell Biology* 20(3):294-302.

Lagouge M, Argmann C, Gerhart-Hines Z, Meziane H, Lerin C, Daussin F, Messadeq N, Milne J, Lambert P, Elliott P, Geny B, Laakso M, Puiqserver P, Auwerx J (2006). Resveratrol improves mitochondrial function and protects against metabolic disease by activating SIRT1 and PGC-1alpha. *Cell* 127:1109–1122.

Li X, Klaus JA, Zhang J, Xu Z, Kibler KK, Andrabi SA, Rao K, Yang ZJ, Dawson TM, Dawson VL, Koehler RC (2010). Contributions of poly(ADP-ribose) polymerase-1 and -2 to nuclear translocation of apoptosis-inducing factor and injury from focal cerebral ischemia. *Journal of Neurochemistry* 113(4):1012-1022.

Lorenz P, Roychowdhury S, Engelmann M, Wolf G, Horn TF (2003). Oxyresveratrol and resveratrol are potent antioxidants and free radical scavengers: effect on nitrosative and oxidative stress derived from microglial cells. *Nitric Oxide* 9(2):64-76.

Luo J, Nikolaev AY, Imai S, Chen D, Su F, Shiloh A, Guarente L, Gu W (2001). Negative control of p53 by Sir2alpha promotes cell survival under stress. *Cell* 107(2):137-148.

Maeda Y, Hunter TC, Loudy DE, Dave V, Schreiber V, Whitsett JA (2006). PARP-2 Interacts with TTF-1 and Regulates Expression of Surfactant Protein-B. *The Journal of Biological Chemistry* 281(14):9600–9606.

McBurney MW, Yang X, Jardine K, Hixon M, Boekelheide K, Webb JR, Lansdorp PM, Lemieux M (2003). The mammalian SIR2alpha protein has a role in embryogenesis and gametogenesis. *Molecular and Cellular Biology* 23(1):38-54.

McKenna NJ, O'Malley BW (2002). Combinatorial control of gene expression by nuclear receptors and coregulators. *Cell* 108(4):465-474.

Meder VS, Boeglin M, de Murcia G, Schreiber V (2005). PARP-1 and PARP-2 interact with nucleophosmin/B23 and accumulate in transcriptionally active nucleoli. *Journal of Cell Science* 118(Pt 1):211-222.

Ménissier-de Murcia J, Molinete M, Gradwohl G, Simonin F, de Murcia G (1989). Zinc-binding domain of poly(ADP-ribose) polymerase participates in the recognition of single strand breaks on DNA. *Journal of Molecular Biology* 210:229-233.

Ménissier de Murcia J, Ricoul M, Tartier L, Niedergang C, Huber A, Dantzer F, Schreiber V, Amé JC, Dierich A, LeMeur M, Sabatier L, Chambon P, de Murcia G (2003). Functional interaction between PARP-1 and PARP-2 in chromosome stability and embryonic development in mouse. *The EMBO Journal* 22(9):2255-2263.

Meyer-Ficca ML, Lonchar JD, Ihara M, Meistrich ML, Austin CA, Meyer RG (2011). Poly(ADP-ribose) polymerases PARP1 and PARP2 modulate topoisomerase II beta (TOP2B) function during chromatin condensation in mouse spermiogenesis. *Biology of Reproduction* 84(5):900-909.

Michan S, Sinclair D (2007). Sirtuins in mammals: insights into their biological function. *The Biochemical Journal* 404(1):1-13.

Milne JC, Lambert PD, Schenk S, Carney DP, Smith JJ, Gagne DJ, Jin L, Boss O, Perni RB, Vu CB, Bemis JE, Xie R, Disch JS, Ng PY, Nunes JJ, Lynch AV, Yang H, Galonek H, Israelian K, Choy W, Iffland A, Lavu S, Medvedik O, Sinclair DA, Olefsky JM, Jirousek MR, Elliott PJ, Westphal CH (2007). Small molecule activators of SIRT1 as therapeutics for the treatment of type 2 diabetes. *Nature* 450(7170):712-716.

Miwa M, Sugimura T (1984). Structure of poly(ADP-ribose). *Methods in enzymology* 106: 441-450.

Moroni F, Formentini L, Gerace E, Camaioni E, Pellegrini-Giampietro DE, Chiarugi A, Pellicciari R (2009). Selective PARP-2 inhibitors increase apoptosis in hippocampal slices but protect cortical cells in models of post-iscaemic brain damage. *British journal of Pharmacology* 157:854-862.

Morris KC, Lin HW, Thompson JW, Perez-Pinzon MA (2011). Pathways for ischemic cytoprotection: role of sirtuins in caloric restriction, resveratrol, and ischemic preconditioning. *Journal of Cerebral Blood Flow and Metabolism* 31(4):1003-1019.

Mortusewicz O, Amé JC, Schreiber V, Leonhardt H (2007). Feedback-regulated poly(ADP-ribosyl)ation by PARP-1 is required for rapid response to DNA damage in living cells. *Nucleic Acids Research* 35(22):7665-7675.

Mota RA, Sánchez-Bueno F, Saenz L, Hernández-Espinosa D, Jimeno J, Tornel PL, Martínez-Torrano A, Ramírez P, Parrilla P, Yélamos J (2005). Inhibition of poly(ADP-ribose) polymerase attenuates the severity of acute pancreatitis and associated lung injury. *Laboratory Investigation* 85(10):1250-1262.

Moynihan KA, Grimm AA, Plueger MM, Bernal-Mizrachi E, Ford E, Cras-Méneur C, Permutt MA, Imai S (2005). Increased dosage of mammalian Sir2 in pancreatic beta cells enhances glucose-stimulated insulin secretion in mice. *Cell Metabolism* 2(2):105-117.

Murata T, Yamawaki H, Yoshimoto R, Hori M, Sato K, Ozaki H, Karaki H (2001). Chronic effect of doxorubicin on vascular endothelium assessed by organ culture study. *Life Sciences* 69(22):2685-2695.

Nemoto S, Fergusson MM, Finkel T (2004). Nutrient availability regulates SIRT1 through a forkhead-dependent pathway. *Science* 306(5704):2105-2108.

Nicolás L, Martínez C, Baró C, Rodríguez M, Baroja-Mazo A, Sole F, Flores JM, Ampurdanés C, Dantzer F, Martin-Caballero J, Aparicio P, Yelamos J (2010). Loss of poly(ADP-ribose) polymerase-2 leads to rapid development of spontaneous T-cell lymphomas in p53-deficient mice. *Oncogene* 29(19):2877-2883.

Oliver AW, Amé JC, Roe SM, Good V, de Murcia G, Pearl LH (2004). Crystal structure of the catalytic fragment of murine poly(ADP-ribose) polymerase-2. *Nucleic Acids Research* 32(2):456-464.

Pacher P, Liaudet L, Bai P, Virag L, Mabley JG, Hasko G, Szabo C. (2002). Activation of poly(ADP-ribose) polymerase contributes to development of doxorubicin-induced heart failure. *The Journal of pharmacology and experimental therapeutics* 300:862-867.

Pacher P, Liaudet L, Bai P, Mabley JG, Kaminski PM, Virág L, Deb A, Szabó E, Ungvári Z, Wolin MS, Groves JT, Szabó C (2003). Potent metalloporphyrin peroxynitrite decomposition catalyst protects against the development of doxorubicin-induced cardiac dysfunction. *Circulation* 107(6):896-904.

Pacher P, Liaudet L, Mabley JG, Cziraki A, Hasko G, Szabo C (2006). Beneficial effects of a novel ultrapotent poly(ADP-ribose) polymerase inhibitor in murine models of heart failure. *International Journal of Molecular Medicine* 17:369-375.

Pacholec M, Bleasdale JE, Chrunyk B, Cunningham D, Flynn D, Garofalo RS, Griffith D, Griffor M, Loulakis P, Pabst B, Qiu X, Stockman B, Thanabal V, Varghese A, Ward J, Withka J, Ahn K (2010). SRT1720, SRT2183, SRT1460, and resveratrol are not direct activators of SIRT1. *The Journal of Biological Chemistry* 285(11):8340-8351.

Panickar KS, Anderson RA (2011). Effect of polyphenols on oxidative stress and mitochondrial dysfunction in neuronal death and brain edema in cerebral ischemia. *International Journal of Molecular Sciences* 12(11):8181-8207.

Pellicciari R, Camaioni E, Costantino G, Formentini L, Sabbatini P, Venturoni F, Eren G, Bellocchi D, Chiarugi A, Moroni F (2008). On the way to selective PARP-2 inhibitors. Design, synthesis, and preliminary evaluation of a series of isoquinolinone derivatives. *ChemMedChem* 3(6):914-923.

Peralta-Leal A, Rodríguez-Vargas JM, Aguilar-Quesada R, Rodríguez MI, Linares JL, de Almodóvar MR, Oliver FJ (2009). PARP inhibitors: new partners in the therapy of cancer and inflammatory diseases. *Free Radical Biology and Medicine* 47(1):13-26.

Phulwani NK, Kielian T (2008). Poly (ADP-ribose) polymerases (PARPs) 1-3 regulate astrocyte activation. *Journal of Neurochemistry* 106(2):578-590.

Picard F, Kurtev M, Chung N, Topark-Ngarm A, Senawong T, Machado De Oliveira R, Leid M, McBurney MW, Guarente L (2004). Sirt1 promotes fat mobilization in white adipocytes by repressing PPAR-gamma. *Nature* 429(6993):771-776.

Pillai JB, Isbatan A, Imai S, Gupta MP (2005). Poly(ADP-ribose) polymerase-1-dependent cardiac myocyte cell death during heart failure is mediated by NAD+ depletion and reduced Sir2alpha deacetylase activity. *The Journal of Biological Chemistry* 280:43121–43130.

Popoff I, Jijon H, Monia B, Tavernini M, Ma M, McKay R, Madsen K (2002). Antisense oligonucleotides to poly(ADP-ribose) polymerase-2 ameliorate colitis in interleukin-10-deficient mice. *The Journal of Pharmacology and Experimental Therapeutics* 303:1145-1154.

Quénet D, El Ramy R, Schreiber V, Dantzer F (2009). The role of poly(ADP-ribosyl)ation in epigenetic events. *The International Journal of Biochemistry and Cell Biology* 41(1):60-65.

Quénet D, Gasser V, Fouillen L, Cammas F, Sanglier-Cianferani S, Losson R, Dantzer F (2008). The histone subcode: poly(ADP-ribose) polymerase-1 (Parp-1) and Parp-2 control cell

differentiation by regulating the transcriptional intermediary factor TIF1beta and the heterochromatin protein HP1alpha. *FASEB Journal* 22(11):3853-3865.

Rajamohan SB, Pillai VB, Gupta M, Sundaresan NR, Birukov KG, Samant S, Hottiger MO, Gupta MP (2009). SIRT1 promotes cell survival under stress by deacetylation-dependent deactivation of poly (ADP-ribose) polymerase 1. *Molecular and Cellular Biology* 29:4116–4129.

Rodgers JT, Lerin C, Haas W, Gygi SP, Spiegelman BM, Puigserver P (2005). Nutrient control of glucose homeostasis through a complex of PGC-1alpha and SIRT1. *Nature* 434:113–118.

Rulten SL, Fisher AE, Robert I, Zuma MC, Rouleau M, Ju L, Poirier G, Reina-San-Martin B, Caldecott KW (2011). PARP-3 and APLF function together to accelerate nonhomologous end-joining. *Molecular Cell* 41(1):33-45.

Sauve AA (2009). Pharmaceutical strategies for activating sirtuins. *Current Pharmaceutical Design* 15:45–56.

Saxena A, Wong L, Kalitsis P, Earle E, Shaffer LG, Choo A. (2002). Poly(ADP-ribose) polymerase 2 localizes to mammalian active centromeres and interacts with PARP-1, Cenpa, Cenpb and Bub3, but not Cenpc. *Human Molecular Genetics* 11(19):2319–2329.

Scarlett JL, Sheard PW, Hughes G, Ledgerwood EC, Ku HH, Murphy MP. (2000). Changes in mitochondrial membrane potential during staurosporine-induced apoptosis in Jurkat cells. *FEBS Letters* 4750:267-272.

Schreiber V, Amé JC, Dollé P, Schultz I, Rinaldi B, Fraulob V, Ménissier-de Murcia J, de Murcia G (2002). Poly(ADP-ribose) polymerase-2 (PARP-2) is required for efficient base excision DNA repair in association with PARP-1 and XRCC1. *The Journal of Biological Chemistry* 277(25):23028-23036.

Schreiber V, Ricoul M, Amé JC, Dantzer F, Meder V, Spenlehauer C, Stiegler P, Niedergang C, Sabatier L, Favaudon V, Ménissier-de Murcia J, de Murcia G. PARP-2: Structure-Function Relationship (2004). *Poly(ADPribosyl)ation*: Chapter 2.

Schreiber V, Dantzer F, Ame JC, de Murcia G. (2006). Poly(ADP-ribose): novel functions for an old molecule. *Nature Reviews Molecular Cell Biololgy* 7(7):517-528.

Shall S (1984). Inhibition of DNA repair by inhibitors of nuclear ADP-ribosyl transferase. *Nucleic Acids Symposium Series* 13:143-191.

Shieh WM, Amé JC, Wilson MV, Wang ZQ, Koh DW, Jacobson MK, Jacobson EL (1998). Poly(ADP-ribose) polymerase null mouse cells synthesize ADP-ribose polymers. *The Journal of Biological Chemistry* 273:30069-30072.

Sims JL., Berger SJ., Berger NA. (1981). Effects of nicotinamide on NAD and poly(ADP-ribose) metabolism in DNA-damaged human lymphocytes. *Journal of supramolecular structure and cellular biochemistry* 16:281-288.

Singal PK, Iliskovic N (1998). Doxorubicin-induced cardiomyopathy. *New England Journal of Medicine* 339(13):900-905.

Smith JS (2002). Human Sir2 and the „silencing" of p53 activity. *Trends in Cell Biology* 12:404-406.

Sunderland PT, Woon EC, Dhami A, Bergin AB, Mahon MF, Wood PJ, Jones LA, Tully SR, Lloyd MD, Thompson AS, Javaid H, Martin NM, Threadgill MD (2011). 5-Benzamidoisoquinolin-1-ones and 5-(ω-carboxyalkyl)isoquinolin-1-ones as isoform-selective inhibitors of poly(ADP-ribose) polymerase 2 (PARP-2). *Journal of Medicinal Chemistry* 54(7):2049-2059.

Tao R., Karliner JS., Simonis U., Zheng J., Zhang J., Honbo N. et al. (2007) Pyrroloquinoline quinone preserves mitochondrial function and prevents oxidative injury in adult rat cardiac myocytes. *Biochemical and Biophysical Research Communications* 363:257–262.

Troiani S, Lupi R, Perego R, Depaolini SR, Thieffine S, Bosotti R, Rusconi L (2011). Identification of candidate substrates for poly(ADP-ribose) polymerase-2 (PARP2) in the

absence of DNA damage using high-density protein microarrays. *FEBS Journal* 278(19):3676-3687.

Virág L, Szabó C (2002). The therapeutic potential of poly(ADP-ribose) polymerase inhibitors. *Pharmacological Reviews* 54(3):375-429.

Wen Y, Li W, Poteet EC, Xie L, Tan C, Yan LJ, Ju X, Liu R, Qian H, Marvin MA, Goldberg MS, She H, Mao Z, Simpkins JW, Yang SH (2011). Alternative mitochondrial electron transfer as a novel strategy for neuroprotection. *The Journal of Biological Chemistry* 286(18):16504-16515.

Xu M, Ashraf M (2002) Melatonin protection against lethal myocyte injury induced by doxorubicin as reflected by effects on mitochondrial membrane potential. *Journal of Molecular and Cellular Cardiology* 3:75–79.

Yang T, Sauve AA (2006). NAD metabolism and sirtuins: metabolic regulation of protein deacetylation in stress and toxicity. *AAPS Journal* 8(4):632-643.

Ye R, Zhang X, Kong X, Han J, Yang Q, Zhang Y, Chen Y, Li P, Liu J, Shi M, Xiong L, Zhao G (2011). Ginsenoside Rd attenuates mitochondrial dysfunction and sequential apoptosis after transient focal ischemia. *Neuroscience* 178:169-180.

Yélamos J, Monreal Y, Saenz L, Aguado E, Schreiber V, Mota R, Fuente T, Minguela A, Parrilla P, de Murcia G, Almarza E, Aparicio P, Ménissier-de Murcia J (2006). PARP-2 deficiency affects the survival of $CD4^+CD8^+$ double-positive thymocytes. *The EMBO Journal* 25(18):4350-4360.

Yélamos J, Schreiber V, Dantzer F (2008). Toward specific functions of poly(ADP-ribose) polymerase-2. *Trends in Molecular Medicine* 14(4):169-178.

Yen HC, Oberley TD, Vichitbandha S, Ho YS, St Clair DK. (1996) The protective role of manganese superoxide dismutase against adriamycin-induced acute cardiac toxicity in transgenic mice. *Journal of Clinical Investigation* 98:1253–1260.

Young GS, Choleris E, Lund FE, Kirkland JB (2006). Decreased cADPR and increased NAD^+ in the $CD38^{-/-}$ mouse. *Biochemical and Biophysical Research Communications* 346(1):188-192.

Yu SW, Wang H, Poitras MF, Coombs C, Bowers WJ, Federoff HJ, Poirier GG, Dawson TM, Dawson VL (2002). Mediation of poly(ADP-ribose) polymerase-1-dependent cell death by apoptosis-inducing factor. *Science* 297(5579):259-263.

Zhang C, Feng Y, Qu S, Wei X, Zhu H, Luo Q, Liu M, Chen G, Xiao X (2011). Resveratrol attenuates doxorubicin-induced cardiomyocyte apoptosis in mice through SIRT1-mediated deacetylation of p53. *Cardiovascular Research* 90:538-545.

11. KEYWORDS

PARP-2, SIRT1, mitochondria, mitochondrial biogenesis, transcription, doxorubicin, vascular damage, vascular smooth muscle, PARP inhibitors

12. ACKNOWLEDGEMENT

I am particularly grateful to my supervisor Dr. Péter Bay for his ceaseless support and guidance during the years of my Ph.D. education.

I would also like to thank Prof. Pál Gergely, head of the Department of Medical Chemistry for giving me all the support for my work.

I am thankful to Prof. László Virág, head of laboratory for the opportunity and place for me to work.

Many thanks to all working at the Department, especially to the members of our laboratory: Dr. Attila Brunyánszki, Dr. Csaba Hegedűs, Dr. Katalin Erdélyi, Petra Lakatos, Katalin Kovács and Dr. Edina Bakondi for their scientific and personal support.

I am much obliged to Ms. Julianna Hunyadi, Mrs. Erzsébet Herbály and Mrs. Anita Jeney Szabó for their excellent technical assistance.

I appreciate the contribution of Dr. Ibolya Rutkai and Dr. Attila Tóth to our scientific publication.

I would like to thank my husband, Csaba Zajdó not only his personal support but also his invaluable contribution to the creating of figures.

Last but not least I would like to thank all who encouraged me during the period of achieving my Ph.D.

13. APPENDIX

The thesis is based on the following publications:

Bai P, Canto C, Brunyánszki A, Huber A, **Szántó M**, Cen Y, Yamamoto H, Houten SM, Kiss B, Oudart H, Gergely P, Menissier-de Murcia J, Schreiber V, Sauve AA, Auwerx J (2011). PARP-2 regulates SIRT1 expression and whole-body energy expenditure. *Cell Metabolism* 13(4):450-60.
IF: 18.207 (2010)

Szántó M, Rutkai I, Hegedűs C, Czikora Á, Rózsahegyi M, Kiss B, Virág L, Gergely P, Tóth A, Bai P (2011). Poly(ADP-ribose) polymerase-2 depletion reduces doxorubicin-induced damage through SIRT1 induction. *Cardiovascular Research* 92(3):430-8.
IF: 6.051 (2010)

Register Number: DEENKÉTK /103/2012.
Item Number:
Subject: Ph.D. List of Publications

Candidate: Magdolna Szántó

Neptun ID: CBEJ25

Doctoral School: Doctoral School of Molecular Medicine

List of publications related to the dissertation

1. Bai, P., Cantó, C., Brunyánszki, A., Huber, A., **Szántó, M.**, Cen, Y., Yamamoto, H., Houten, S.M., Kiss, B., Oudart, H., Gergely, P., Menissier-de, M.J., Schreiber, V., Sauve, A.A., Auwerx, J.: PARP-2 regulates SIRT1 expression and whole-body energy expenditure.
Cell Metab. 13 (4), 450-460, 2011.
IF:18.207 (2010)

*2. **Szántó, M.**, Rutkai, I., Hegedűs, C., Czikora, Á., Rózsahegyi, M., Kiss, B., Virág, L., Gergely, P., Tóth, A., Bai, P.: Poly(ADP-ribose) polymerase-2 depletion reduces doxorubicin-induced damage through SIRT1 induction.
Cardiovasc. Res. 92 (3), 430-438, 2011.
DOI: http://dx.doi.org/10.1093/cvr/cvr246
IF:6.051 (2010)

*The article dually serves as the basis of dissertation. First writer to cite the article was Ibolya Rutkai (HDBA73)
Statement on th epartial use of article was issued on Dec 8, 2011

List of other publications

3. Brunyánszki, A., Hegedűs, C., **Szántó, M.**, Erdélyi, K., Kovács, K., Schreiber, V., Gergely, S., Kiss, B., Szabó, É., Virág, L., Bai, P.: Genetic ablation of PARP-1 protects against oxazolone-induced contact hypersensitivity by modulating oxidative stress.
J. Invest. Dermatol. 130 (11), 2629-2637, 2010.
DOI: http://dx.doi.org/10.1038/jid.2010.190
IF:6.27

Total IF: 30.528

Total IF (publications related to the dissertation): 24.258

The Candidate's publication data submitted to the Publication Database of the University of Debrecen have been validated by Kenezy Life Sciences Library on the basis of Web of Science, Scopus and Journal Citation Report (Impact Factor) databases.

02 Apr, 2012